

~~FINAL~~
~~ANNUAL~~ REPORT

April 1, 1977
Research Unit - 59

RU-059

✓ Coastal Morphology, Sedimentation
and Oil Spill Vulnerability

Miles O. Hayes - Principal Investigator
Christopher H. Ruby - Co-investigator
Coastal Research Division
University of South Carolina
Columbia, S. C. 29208

Contract No. 03-5-022-82

Notes -

Project 1. Shoreline of the Northern Gulf of Alaska (Hinchinbrook
Island to Dry Bay)

Project 2. Shoreline of Kotzebue Sound (Cape Prince of Wales to
Point Hope)

Task Objectives

The major emphasis of this project **falls** under Task D-Y, which is to: evaluate present rates of change in coastal morphology, with particular **em-phasis** on rates and patterns of man-induced changes and locate areas where coastal morphology is **likely** to be changed by man's activities; and evaluate the effect **of** these changes, if any. The relative susceptibility of different coastal areas **will** be evaluated.

I. Summary of objectives, conclusions and implications with respect to OCS oil and gas **devleopment**

Conclusions regarding the vulnerability of the various environments of the **Gulf** of Alaska-are **presented** in detail in the first paper, "Potential Oil Spill Impacts"? by Miles O. Hayes **and** Christopher H. Ruby, of this report. Very briefly, they indicate that slightly more than 50% of the 1773.4 kms of shoreline classified are considered high. **riskenvironments. Oil would remain in** these areas for periods of time ranging from a few years to as much as 10 years.

In the second section of this report, "Sedimentology" by Christopher H. Ruby, detailed **sedimentological** analysis of the 400+ sediment samples collected is presented. This section is followed by an appendix which contains the grain size data as **well** as compositional data. Briefly, the grain size and compositional trends agree with the transport trends detailed in **Nummedal** and Stephen's progress report "Coastal Dynamics and Sediment **Transportation**, Northeast Gulf of Alaska".

II. Introduction

This report is broken into two subdivisions. The first, Project 1, dealing with the Gulf of Alaska, contains the two sections mentioned above. The second, Project 2, deals with ongoing research in the **Kotzebue** Sound area.

III. Current state of knowledge

This is discussed in each of the individual sections.

IV. Study area

Located in Figure 8 of "Potential Oil **Spill** Impacts" section.

V. Sources, methods and rational of data collection

This is discussed in **detail** in each of the individual sections.

VI. Results

The results are discussed in detail in each section. Topographic maps of the study area with an oil vulnerability risk classification overlay are provided in a folder following this report. In addition, magnetic tapes containing grain size data and beach profile data are being submitted under separate cover.

VII. Discussion and VIII Conclusions

Included in individual reports.

IX. Needs for further study

Two requests for extensions in funding have been submitted: One for Bristol Bay consisting of 1) Geomorphic **classification**, 2) **Sedimentological** study, 3) **Oil spill** vulnerability, and 4) Hydrography associated with tidal sand bodies. The second pertains to an ice study of the **Kotzebue** Sound area and its interaction on potential oil spills in the area.

X. Summary of 4th quarter operation

Detailed under each project section.

Project 1. Shoreline of the Northern Gulf of Alaska (**Hinchinbrook** Island to Dry Bay).

a) Field and Laboratory Activities

No field work has been carried out on this project since the 1975 field session. **All** laboratory analyses of sediment samples have been completed for both textural and compositional parameters. Our **main** emphasis, at this time, is placed on completion of our analysis of the coastal morphology of the study area.

b) Results

The results are presented in the two sections below. **They** are:

1. **Potential** Oil Spill Impacts by Miles O. Hayes and Christopher H. Ruby.

2. Sedimentology by Christopher H. Ruby.

The first section utilizes an oil vulnerability scale devised by our Oil Spill Assessment Team (OSAT) to delineate the relative impact of **potential** oil **spills** on the various coastal environments in the Northern Gulf of Alaska. The second **section** presents a detailed analysis of **sedimentological** trends on the beaches of the **study area**. Both textural and compositional parameters have been used to delineate these trends. The raw compositional and textural data are given in an appendix included at the end of the Sedimentology section. Additionally, magnetic tapes are being submitted under separate cover. These tapes contain the grain size data and **the** beach profile data in the formats developed by NODC.

POTENTIAL OIL SPILL IMPACTS

Miles O. Hayes
Christopher H. Ruby

Introduction

As **oil** exploration and development continue to escalate in Alaska, the potential for **oil** spills in the coastal environment increases. The **Trans-Alaska** Pipeline, soon to be operative, will open a new era with regard to petroleum transport via tankers in Alaskan coastal waters. These tankers will operate on a route between the west coast of the lower 48 states and **Valdez**. This route will take them into the coastal waters on the western edge of the study area where it borders Prince William Sound. In addition, exploration is rapidly advancing in the Gulf of **Alaska** itself. Any production facilities and their support facilities located **in** the Gulf would subject the adjacent shorelines to potential oil spills. Large spills or chronic small **spillages** could result in serious environmental damage. Estuarine and open marine assemblages could be seriously affected by oil spills and clean-up efforts, thus reducing or eliminating their productivity, and, therefore, affecting the food chain. It is unclear, at this **time**, what effect oil **spills** would have on economic species harvested by the numerous fishing villages within the area. Trends in sedimentation can also be altered by oil spills. Some of the more sensitive geomorphic environments can retain spilled oil for periods of time **ranging** to 10 years. Thus, development of this area will require careful evaluation of the possible impacts of potential oil spills.

Case Studies

Introduction. - The Coastal Research Division has developed an **interdisciplinary** Oil Spill Assessment Team (OSAT). During the past two years, they have had the opportunity to study two major oil spills in considerable detail and three moderate spills in slightly less detail (Table 1). The authors are members of

TABLE 1: MAJOR OIL SPILLS STUDIED BY OSAT*

<u>Oil Spill</u>	<u>Date</u>	<u>Type & Amount of Oil</u>	<u>Affected Coastline</u>	<u>Control/Treatment Methods</u>	<u>OSAT Field Studies</u>
<u>Metula</u> Strait 'of <u>Magellan</u> , Chile	August 1974	Type: Saudi Arabian Crude 3% Bunker C 53,000 tons total 40,000 tons on coastline	150 km Sand & Gravel Beaches Estuaries Marshes/Tidal Flats	No clean-up or " control activities	12-20 August 1975 4 Feb.-13 March 1976 12-23 August 1976
<u>Urquiola</u> La Coruna, Spain '	May 1976	Type: Persian Gulf Crude 2% Bunker C 110,000 tons total 25-30,000 ashore	215 km Sandy Beaches Rocky Shores Estuaries Marshes/Tidal Flats	Dispersants Booms and Pumps Heavy Machinery Manual Labor '	17 May-10 June 1976
<u>Jakob Maersk</u> <u>Porto</u> , Portugal	Jan. 1975	Type: Iranian Crude 2% Bunker C 80,000 tons total 15-20,000 tons ashore	Sandy Beaches Rocky Shores Shore Facilities	Dispersants Booms Heavy Machinery Manual Labor	4-6 June 1976
<u>Argo Merchant</u> 17 miles off Nantucket Island, U.S.	Dec. 1976	Type: No. 6 fuel oil 27,000 tons	None	Rough Sea Conditions prevented effective use of control equipment	Overflight 23 Dec. 1976
<u>Bouchard #65</u> Wings Neck Area Buzzards Bay, Mass., U.S.	Jan. 1977	Type: No. 2 fuel oil 275 tons	Approx. 1-2 kms, Fast ice protected beaches	Suction pumps Sorbents Oiled ice removal Burning	30 Jan.-3 Feb. 1977
<u>Ethel H</u> <u>Lower Hudson R.</u> , New York, U.S.	Feb. 1977	Type: No. 6 fuel oil 1500 tons lost	10 km of shoreline Little apparent damage due to fast ice along shoreline	Booms Ice Skimmer (Suction truck on LCM)	7-8 Feb. 1977

*Oil Spill Assessment Team, Coastal Research Division, University of South Carolina

that **team**; however, many of the concepts summarized in this sub-section are the results of interaction by the entire **group**.¹

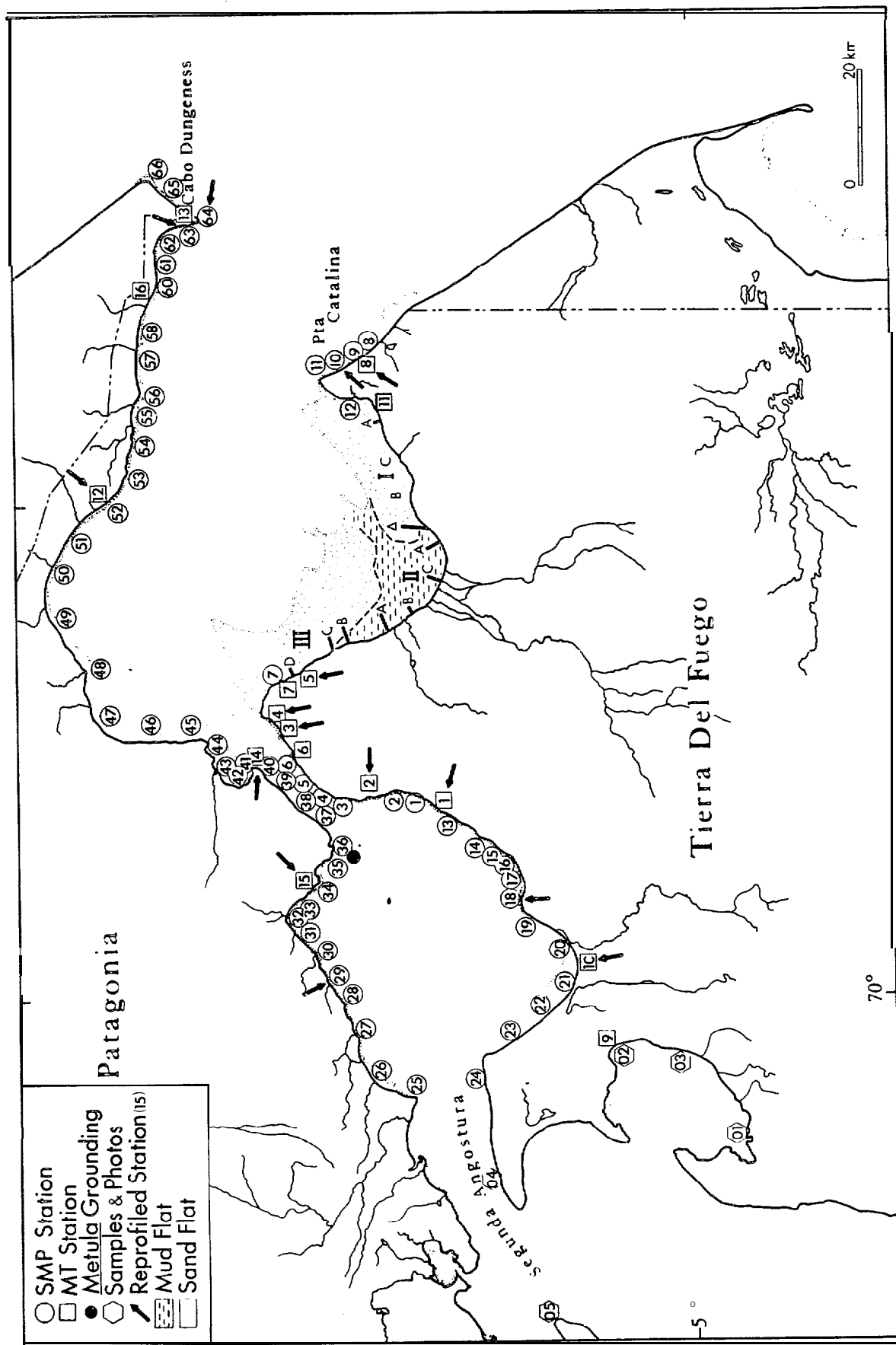
The Metula spill. - The VLCC Metula ran aground on 9 August 1974, while navigating through the eastern passage of the Strait of **Magellan** (Fig. 1). Over the next month, 53,000 tons of oil leaked from the ship, and 40,000 tons washed onto the nearby shores (**Hann**, 1974) . Because of the remoteness of the area and questionable legal responsibility for the accident, no attempt was made to control or clean up any of the spreading oil. We were able to visit the spill site during August 1975 and found that oil coverage was still extensive in many of the coastal environments that were originally affected (Fig. 2), including beach face and **low-tide** terrace portions of gravel and sand beaches, **tidal** flats, marsh areas, and **tidal** channels (**Hayes** and **Gundlach**, 1975; **Hayes et al.**, 1976). Because of the great similarity of the area to the coasts of New England and Alaska, a full study was sponsored by NSF-RANN during January -March, 1976. A total of 66 zonal stations was set up in a manner similar to those in the Gulf of Alaska study area. A geomorphic breakdown was made of the affected area, and the distribution and perseverance of the oil was analyzed within the framework of that breakdown. Sixteen stations were selected as representative areas and studied in much greater detail. Trenches were analyzed to determine **oil** distribution beneath the present beach surface, and plan-view oil distribution maps were superimposed on our **physiographic** maps for each locality. A full report of this spill is now in preparation and will be published sometime this year.

The **oil** distribution on the affected environments assumed many forms primarily as a-result of **process variables** (tide, wave and wind energy) in the particular en-

¹ **Anne E. Blount**
Ian A. Fischer
Erich R. **Gundlach**
Miles O. **Hayes**

Jacqueline **Michel**
Christopher H. **Ruby**
Robert J. **Stein**
Larry G. **Ward**

Figure 1. Metula oil spill site in the Strait of Magellan. Numbers within circles indicate SMP stations which consist of beach profiles, trenches, sediment samples and photo and tape descriptions. Numbers within squares are MT stations which consist of more detailed SMP information plus an oil concentration map superimposed on a geomorphic base map. Photo and sample sites are indicated by open hexagons. Short heavy lines on the sand and mud flats just west of Pta. Catalina represent profiles. This represents part of the data base developed by the Metula oil spill field teams.



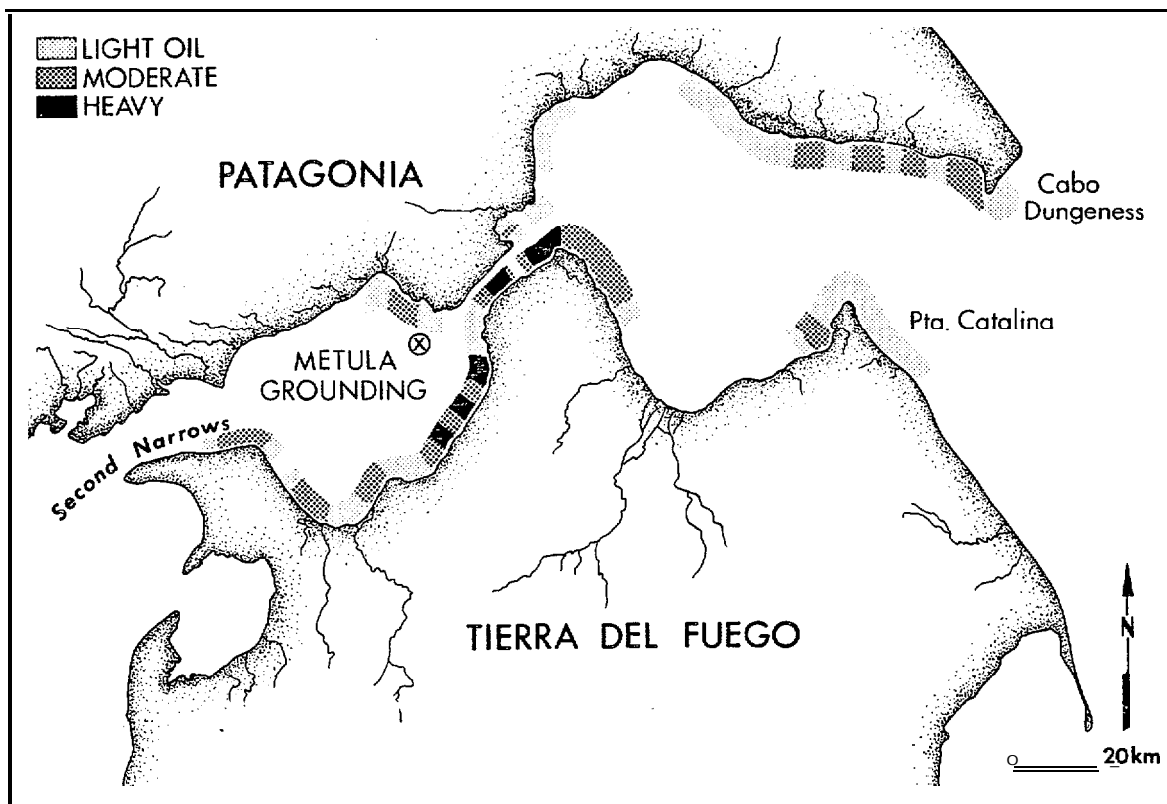


Figure 2. Oil concentration map of the Metula oil spill site in the Strait of Magellan. This represents the relative concentration of oil within the beach zone 18-months after the spill. Oil was moved primarily by the strong westerly winds and tidal currents.

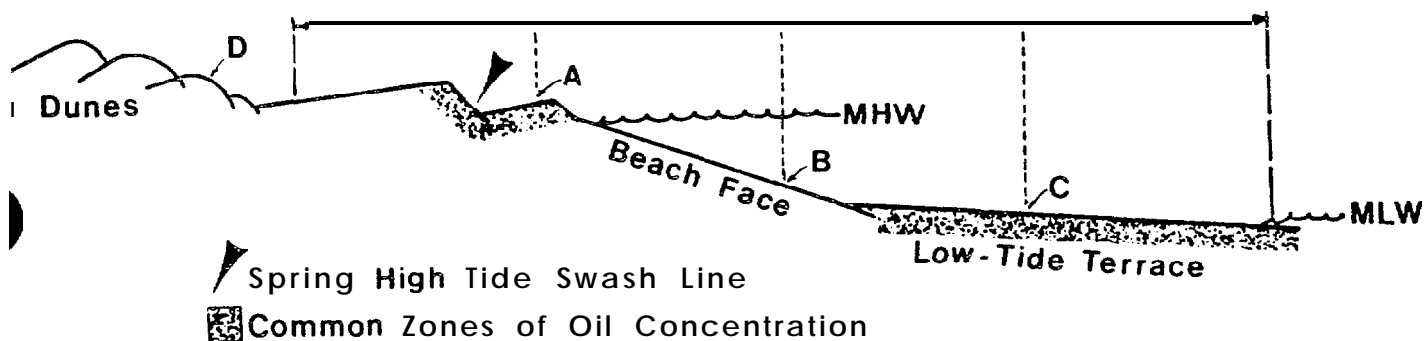


Figure 3. Typical beach profile for the Metula impact site. Letters indicate sampling localities, which are located between the upper limit of normal high waves and the low water line. B is in the center of the sampling zone, and stations A and C are located at the midpoint of the upper and lower halves of the sampling zone. D is usually a dune sample. A core sample 15 cm in length is taken at each station.

vironments and the topographic setting. On open beaches, the oil was generally deposited on the surface of berm top overwashes or at the high tide swash lines, and often at the base of the beach face if a low-tide terrace was present (Fig. 3).

In the mid-beach face, the oil was either never deposited, deposited and later eroded, or buried beneath more recent beach deposits usually in the form of berms. Sheltered tidal flats and salt marshes, where the oil was still present in much the same form as when it was deposited, were by far the most severely impacted areas (Fig. 4). Large pools of oil covered most of the meandering tidal channels, killing much of the vegetation and covering a large percentage of the marsh surface with a thick (a few centimeters) layer of oil. Gravel accumulations, due to their very high permeability, were also highly affected. In some areas, the gravels and sand had been mixed with the oil to form a "blacktop" which was extremely resistant to erosion,

The Metula spill site presents an exceptional analogue for many of the areas in the Gulf of Alaska study area. Similar tidal range, recent geologic history, and sediment types make the oil behavior documented at the Metula site an ideal comparative tool for predictive purposes in this Alaskan study.

Figure 4. A. Aerial view of the meandering tidal channels in the East Estuary on the first Narrows, Strait of Magellan. Oil spilled by the Metula can be seen as glossy areas fringing the channels, (arrows). Oil thickness ranged to 10 cm. Deposition of this oil took place during spring high tides, washing" the oil over the levee bordering the channels, and into the marsh. Much of the vegetation was devastated by the oil.

Figure 4. B. Ground view of a tidal channel in the East Estuary marsh. Arrows indicate heavy oil accumulations washed out of the channels. Man on the left stands at the edge of this heavy accumulation. Note that the vegetation around the oil has been killed. This photo was taken 18 months after the oil spill. We estimate a 10 year life span for this oil.

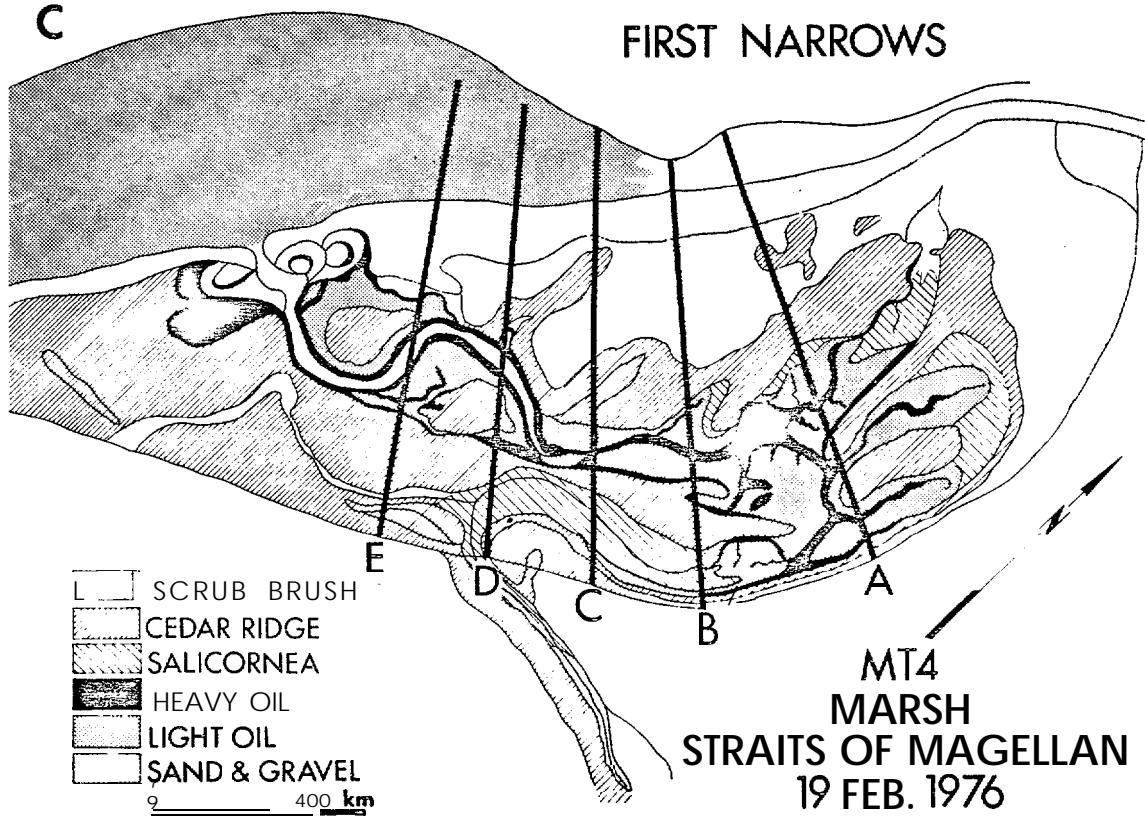
Figure 4. C. Map of East Estuary showing zones of oil accumulation. Heavy lines indicate transit profiles across the marsh system. Note the oil accumulations fringing the marsh channels and on the low tide terrace on the upper left of the map.



B



C



The Urquiola spill. - at 8:00 a.m., 12 May, 1976, the supertanker Urquiola ran aground at the entrance to La Coruna harbor in northwestern Spain. The ship exploded in the early afternoon. Part of its cargo of 100,000 tons of crude oil burned, but approximately 25-30,000 tons washed into the coastal environments of this classic "Ria" system. After 9 days, the oil had dispersed over 60 km of coastline. One month after the grounding, a total of 215 km of coastline had been impacted by the oil.

A preliminary study of the Urquiola spill was carried out by the authors and 5 associates immediately after the spill, from 17 May through 10 June 1976. Many different coastal environments were affected by the spilled oil. The area classified as a Ria system (flooded river valleys) has numerous rock headlands protecting quieter embayments. Bay mouth bars are common in the inner reaches of the rias, protecting tidal flat and marsh complexes behind them.

It was found that floating oil masses did not contaminate the rock headlands due to their exposed character, Waves reflecting from the rock cliffs kept the oil mass a few meters from the rocks. Even where oil splashed onto the cliffs, the intense wave attack soon cleaned them. However, on rock scarps within the rias, the lower wave energies permitted the oil to coat the rocks, where it will remain for a variable period of time dependent on the intensity of wave and tidal action. On the fine sand beaches within the rias, heavy deposition of oil took place, devastating infauna. However, the fine compact nature of the sediment did not permit penetration of the oil to more than a few centimeters, thus repeated wave attack should clear the beaches within a few months. This type of beach also lends itself to mechanized clean-up. For a complete discussion of mechanized clean-up methods for beaches, the reader is referred to Sartor and Foget (1971). Within the tidal flats and marshes, oil pollution was considerably worse. Oil entered these areas primarily via tidal currents and once into the marsh, it tended to adhere to the marsh vegetation. It sank into burrows of the abundant infauna often with devastating biological impact. The extremely fine grain size of the marsh and tidal flat sediments prevents direct penetration of the oil to a depth of more than a centimeter or two; thus most of

the oil remains on the surface where it is reactivated by each tide and moved from one area to another. This results in repeated contamination of areas within the marsh-tidal flat system. Two primary factors make these areas extremely sensitive to oil spill damage:

- 1) The biomass of these areas is high. They are breeding grounds for many economic species as well as habitats for juvenile forms of economically important fin and shellfish. In addition, large populations of infauna exist within these areas.
- 2) The relatively low energies (tides, winds, waves, etc.) in these areas result in very long residence times for the oil. Degradation of the oil is often orders of magnitude slower than on exposed sections of coast.

Finally, there were a small number of exposed sand beaches, both north and south of the Ria system, which were contaminated by oil. Although they received a heavy dose of the oil, the high wave energies present tended to re-work the sediments, resulting in a natural cleansing of the beach. These areas should clean themselves within a few months. Figures 5 through 7 show some of the environments contaminated by the Urquiola oil spill.

These two oil spills, plus the analysis of numerous other spills in the literature, all point the obvious fact that the physical degradation of the oil is directly related to the energy in the environment where the oil is deposited. Table 2, from Rashid (1974), gives supportive quantitative data in this regard.

Cold water spills. - There is abundant literature dealing with case studies of the numerous major and minor oil spills that have taken place in coastal waters of the lower 48 states. Predictive models for oil spill dispersal, spreading, biodegradation and physical degradation have been developed from these studies. The Arctic and sub-Arctic areas, however, have been to a large extent omitted due to the difficulties inherent in any study of these environments and a general lack of actual oil spills in these environments from which to base detailed case studies. The Arrow oil spill in Chedabucto Bay, Nova Scotia, probably comes closest to a comparative model for the sub-Arctic. However, the clean-up effort and later studies (Owens

Figure 5 A. Fine sand beach near La **Coruna**, Spain, oiled by the Urquiola oil spill. Oil covers the beach from the present swash zone to the high tide **swash**. Note the erosion of the **oil** at the present swash line (arrow). The fine grained nature of this beach has prevented the penetration of the oil. Most of the oil **should** be cleaned by natural processes **withn** six months.

Figure 5 B. Photo of a trench in a mixed sand beach. The lower **unit in the** trench is composed of coarse sand deposited during spring tides. The spilled oil then polluted the beach forming a **layer** of mixed sand and oil. Later, a neap berm of finer sand was deposited on top of the oiled layer, resulting in some erosion of the oil. Small oil droplets can be seen as a swash line on the present beach face. Scale is 15 cm.

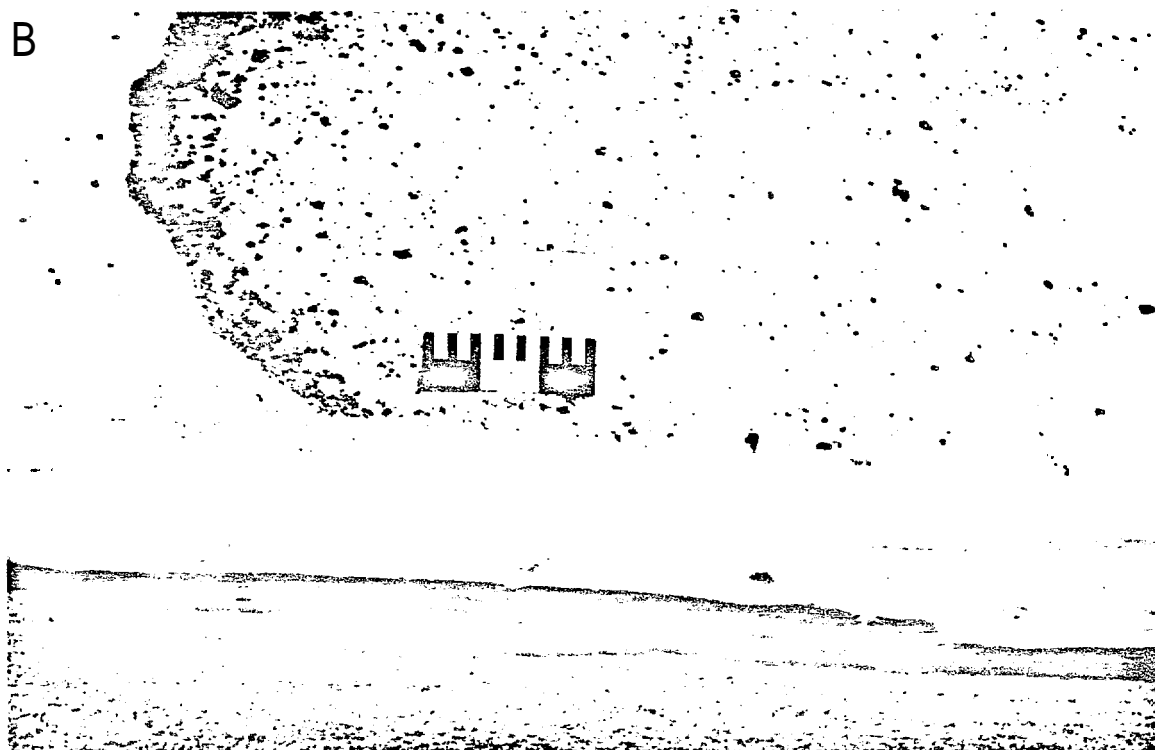


Figure 6. A. This photo of a coarse sand beach in the La Coruna area displays two prominent oil concentrations (arrows). This high energy beach has two berms and two berm top overwash areas. These overwash areas act as traps for the oil, resulting in heavy accumulations. The high wave energy at this location should result in rapid natural cleaning (about 6 months).

Figure 6. B. Photo shows a thick deposit of mixed sand and oil on a low-tide terrace at the toe of the beach face. This is a common zone of oil accumulation. The high wave energies at this location have eroded most of the oil. In addition, the fine grained nature of the sediments prevented penetration of the oil.

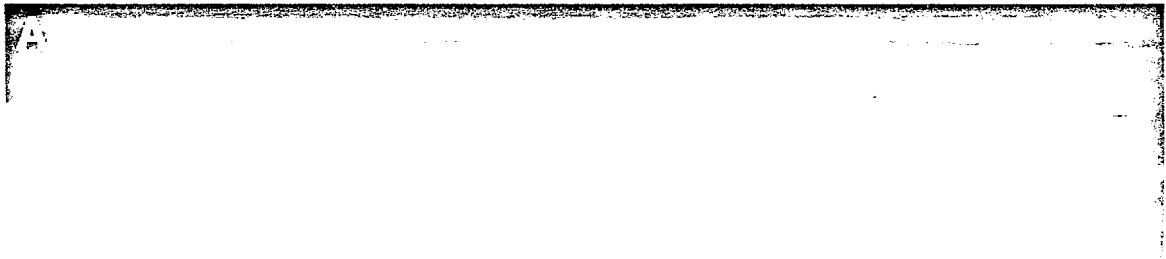




Figure 7. This small pocket beach in the La Coruna area shows the variable impact of oil pollution on sediments of different grain size. The high tide swash line on the gravels is evident to the left (arrow). The oil left a heavy coating on the gravels, but not the sand in the middle of the beach. In addition, the low energy of this pocket beach permitted the oil to leave a coating on the large bedrock outcrops. The relationship of grain size to oil penetration is an extremely important factor to be considered when designing a vulnerability scale.

Table 2. Chemical and physical characteristics of original and residual Bunker C oils extracted from sediments collected in Chedabucto Bay 3½ years after the Arrow spill (from Rashid, 1974).

Characteristics	Bunker C oil Original ^a	Stored sample	Low energy coast	Moderate energy coast	High energy coast
Hydrocarbons (%)					
Saturated	---	26	25	23	18
Aromatic	-.	25	24	24	16
Total hydrocarbons	73.1	51	49	47	34
Ratio of saturate to aromatic	..	1.04	1.04	0.96	1.12
Non-hydrocarbons (%)					
Asphaltenes	16.3	20	22	23	22
Resins and NSOS	10.6	29	29	30	44
Total of non-hydrocarbons	26.9	49	51	53	66
Hydrocarbons/ non-hydrocarbons	2.72	1.04	0.96	0.88	0.52
Physical properties					
Specific gravity	0.950	0.963	0.9953	0.9765	0.9823
Viscosity (cP)		19.584	28.600	1210.000	3640.000

^aTask Force Operation Oil Report, 1970

and **Drapeau**, 1973; Owens, 1973; Drapeau, 1973; Owens, 1971; Owens and Rashid, 1976), made very little reference to the special problems encountered as a result of the colder environment (*i.e.* oil on ice and snow; ice-oil interaction with the beach sediments; oil dispersal in heavily iced waters, etc.). Our investigations of the Buzzards Bay Oil Spill (Ruby *et al.*, in prep.) and the Ethyl H. Oil Spill in the frozen Hudson River (Ruby and **Gundlach**, in prep.), have given new insight into the extremely limiting effects of oil spills in ice-choked waters.

Further, evaporation losses and biodegradation are slower in colder environments. Biodegradation can be reduced as much as 90% in water of 0°C when compared to water of 25°C, (Robertson, 1972). Isakson *et al.*, (1975) states that burning may be the only feasible method of cleaning oil spills in iced areas; however, this simply represents a trade of one type of pollution for another. It did not prove to be an effective clean-up method at the Buzzards Bay oil spill.

Finally, intense tidal currents and winds in the study area can disperse

the spilled oil in an unpredictable manner, making it nearly impossible to recover before it impacts on the shorelines. Drapeau et al., (1970) concluded that it is not feasible to recover or disperse oil slicks in regions of strong tidal currents.

Conclusion. - In summary, the potential for oil spills in the Gulf of Alaska is increasing as exploration and development continue to escalate in the Gulf and other areas of Alaska. There is a very complex interaction of marine processes during an oil spill which can make it extremely difficult to predict the track and dispersal pattern the oil spill will follow. However, numerous case studies permit the construction of an oil spill vulnerability scale which is based on the biologic sensitivity and natural cleaning ability of particular environments. This scale has been applied to lower Cook Inlet (Michel et al., 1977) and is here modified for the Gulf of Alaska.

Environmental Vulnerability to Oil Spills

This scale has been devised on the basis of the case studies summarized above and a careful study of the literature. It is based primarily on the longevity of oil in each sub-environment which is generally a function of the intensity of the marine processes, sediment size and transport trends. The biologic sensitivity has also been utilized to modify the ratings of the various environments.

Coastal environments are listed and discussed below in order of increasing vulnerability to oil spills:

1. Straight, rocky headlands:

Most areas of this type are exposed to maximum wave energy. Waves reflect off the rocky scarps with great force, readily dispersing the oil. In fact, waves reflecting off the scarps at high tide tend to generate a surficial return flow that keeps the oil off the rocks (observed at the Urquiola spill site in Spain). Parts of Kayak Island and Hinchinbrook Island fall into this category. Even if oiled, natural cleaning will only require a few days or weeks. No human intervention is necessary.

2. Eroding wave-cut platforms:

These areas are also swept clean by wave erosion. All of the areas of this type at the Metula spill site had been cleaned of oil after one year. The rate of removal of the oil is a function of wave climate. In general, no clean-up procedures are needed for this type of coast. Kayak Island, Hinchinbrook Island, and Point Riou have wave-cut platforms.

3. Flat, fine-grained sandy beaches:

Beaches of this type are generally flat and hard-packed. Oil that is emplaced on such beaches will not penetrate more than a few centimeters at most. Usually, the oil will be deposited on the surface of the sand where it can be easily removed by elevated scrapers or other road grading machinery. Furthermore, these types of beaches change slowly, so sand deposition and resultant burial of oil will take place at a slow rate. If left to natural processes, these beaches will be cleaned within several months. Much of the Yakutat Forceland and all of the Copper River delta barriers fall into this category.

4. Steeper, medium- to coarse-grained sandy beaches:

On these beaches, the depth of penetration would be greater than for the fine-grained beaches (though still only a few centimeters), but rates of burial of the oil would be greatly increased. Based on earlier studies by our group in numerous localities, it is possible for oil to be buried as much as 50-100 cm within a period of a few days on beaches of this class. In this type of situation, removal of the oil becomes a serious problem, since removal of the oiled sediments will often result in large scale erosion, as the beach changes into a new equilibrium state. This was a common problem encountered during the clean-up of the Arrow spill in Chedabucto Bay, Nova Scotia (Owens and Rashid, 1976). Another problem is that burial of the oil preserves it for release at a later date when the beach erodes as part of the natural beach cycle, thus causing longer term pollution of the environment. Many of the spits

between Cape Suckling and Icy Bay fall into this category.

5. Impermeable muddy tidal flats (exposed to winds and currents):

One of the major surprises of the study of the Metula site was the discovery that oil had not remained on the mud flats. At the Urquiola site, oil was observed as it became refloated with rising tides on the mud flats. Penetration of the oil is prevented by the extremely fine sediment size, saturated with water. Therefore, if an oiled tidal flat is subject to winds and some currents, the oil will tend to be removed, although not at the rapid rate encountered on exposed beaches. Mechanized clean-up is considered impossible. These are often areas of high biologic importance. There are large areas of mud and fine sand tidal flats behind the barriers on the Copper River Delta.

6. Mixed sand and gravel beaches:

On beaches of this type, the oil may penetrate several centimeters, and rates of burial are quite high (a few days in Spain). Again, any attempt to remove the oiled sediment will result in considerable erosion. Most of the beaches between Cape Suckling and Icy Cape are of this type. There are also many beaches within Icy Bay and all along the Malaspina Foreland which are mixes of sand and gravel. The longevity of the oil at the Metula site, particularly on the low-tide terraces and berm top areas, attests to the high susceptibility of this type of beach to long-term oil spill damage. Natural cleaning may require a few years.

7. Gravel beaches:

Pure gravel beaches allow the oil to penetrate to considerable depth (up to 45 cm in Spain). Furthermore, rapid burial is also possible. A heavily-oiled gravel beach will be impossible to clean up without completely removing the gravel. Natural cleaning will be quite slow for this type of beach; the exact time required will depend on the intensity of the marine processes. There are pure gravel beaches within both Icy Bay and Yakutat Bay (both under consideration as harbor sites). The bays are quite sheltered, and, thus, spilled oil will remain for periods of at least

a few years in these bays. The beaches just east of Sitkagi Bluffs are also composed of pure gravel; however, their exposed nature will result in considerably more rapid natural cleaning.

9. Sheltered rocky headlands:

Our experience in Spain indicates that oil tends to stick to rough rocky surfaces. In the absence of abrasion by wave action, oil could remain on such areas for years, with only chemical and biological processes left to degrade it. There are a number of sheltered rock headlands and cliffs within Icy Bay and Yakutat Bay. However, the Elias Mountains, just inland, develop nearly continuous orographic winds blowing from the north across the bays. These winds increase in intensity as the bay heads are approached. Given this wind and its domination over tidal processes, it is considered unlikely that an oil slick could penetrate deeply enough into the bays to damage the rock headlands.

10. Protected estuarine tidal flats:

If oil reaches a quiet, protected estuarine tidal flat, it will remain there for long periods because natural cleaning progresses at an extremely slow rate. Because of the low intensity of marine process parameters, removal of the oil will have to be accomplished by natural chemical and biogenic processes. This will take many years, dependent on the amount of oil deposited. Because of their high populations, these environments are very sensitive to the toxic effects of oil. A number of areas of this type exist on the Copper River Delta and in Controller Bay.

10. Protected estuarine salt marshes:

In sheltered estuaries, oil from a spill may have long-term deleterious effects. We observed oil from the Metula on the salt marshes of East Estuary, in the south shore of the Strait of Magellan, that had shown essentially no change in 1½ years. We predict a life span of at least 10 years for that oil. These areas are extremely important biologically, supporting large communities of organisms. The inner parts of the Copper River Delta contain massive salt marshes.

Applications to the Northern Gulf of Alaska

Oil spill vulnerability. - Utilizing a combination of the vulnerability classification just described and a classification of coastal morphology, it is possible to delineate the coastal environments of the Gulf of Alaska with respect to oil spill vulnerability. Generally, the Gulf is a high risk area especially in the Copper River delta section. Many of the environments have a high risk rating as explained below. In addition, the entire study area is remote and almost inaccessible to standard clean-up operations. Of all the environments, the erosional shorelines in rock **scarps** on **Hinchinbrook** Island and Kayak Island as well as **scarps** into glacial sediments, are most apt to be rapidly cleaned by natural processes. The marsh and tidal flat areas on the Copper River delta and other smaller river mouths are extremely high risk areas. The rest of the beaches of the study area are variable, depending essentially upon the wave energy and beach grain size. Oil burial can be a problem with these sand and gravel Leaches.

Using the ten morphological subdivisions discussed earlier, a risk classification has been devised and applied to the northern Gulf of Alaska study area (Fig. 8). Table 3 shows the results of this application.

Oil longevity within these risk classifications is estimated as follows:

<u>Risk Class</u>	<u>Longevity</u>
1-2	A few days to a few weeks
3-4	A month to six months
5-6	Less than 12 months
7-8	A year or two
9-10	Up to ten years

Table 3

<u>Km of shoreline</u>	<u>% of shoreline</u>	<u>Discussion</u>	<u>Risk Classification</u>
130.4	7	Oil easily removed by wave erosion; some problems in areas of gravel accumulation and pocket beaches, This includes most of the Type 1 and 2 shorelines	1-2
298.5	17	Generally low risk areas. Fine sands prevent penetration of oil. Possibility of oil burial. Most Type 3 and 4 beaches fall into this risk class	3-4
421	24	Mud tidal flats do not permit deep penetration of the oil, but the relatively low energies require as much as a year to remove the oil. Sand and gravel beaches are highly prone to oil burial and thus fall into this risk class. Most beaches of Type 5 and 6 fall into this risk class.	5-6
513.5	29	These areas include mud tidal flats which are highly sheltered as well as sand and/or gravel beaches within bays and sheltered areas. Oil will remain for periods of a few years in these areas. Includes coastal types 7 and 8.	7-8
410	23	These highly sensitive marsh and tidal flat areas can retain oil for up to 10 years. In addition, these areas are of extreme biological importance. Coastal Types 9 and 10 fall into this category.	9-10






Table 3 shows that over half of the 1773.4 kms of shoreline classified fall into the high risk categories of 7-10. Oil longevity in these areas is estimated to be a few years to as much as 10 years. However, some of these high risk areas located on the Copper River delta and other river mouths are unlikely to receive oil spills because of fluvial flushing.

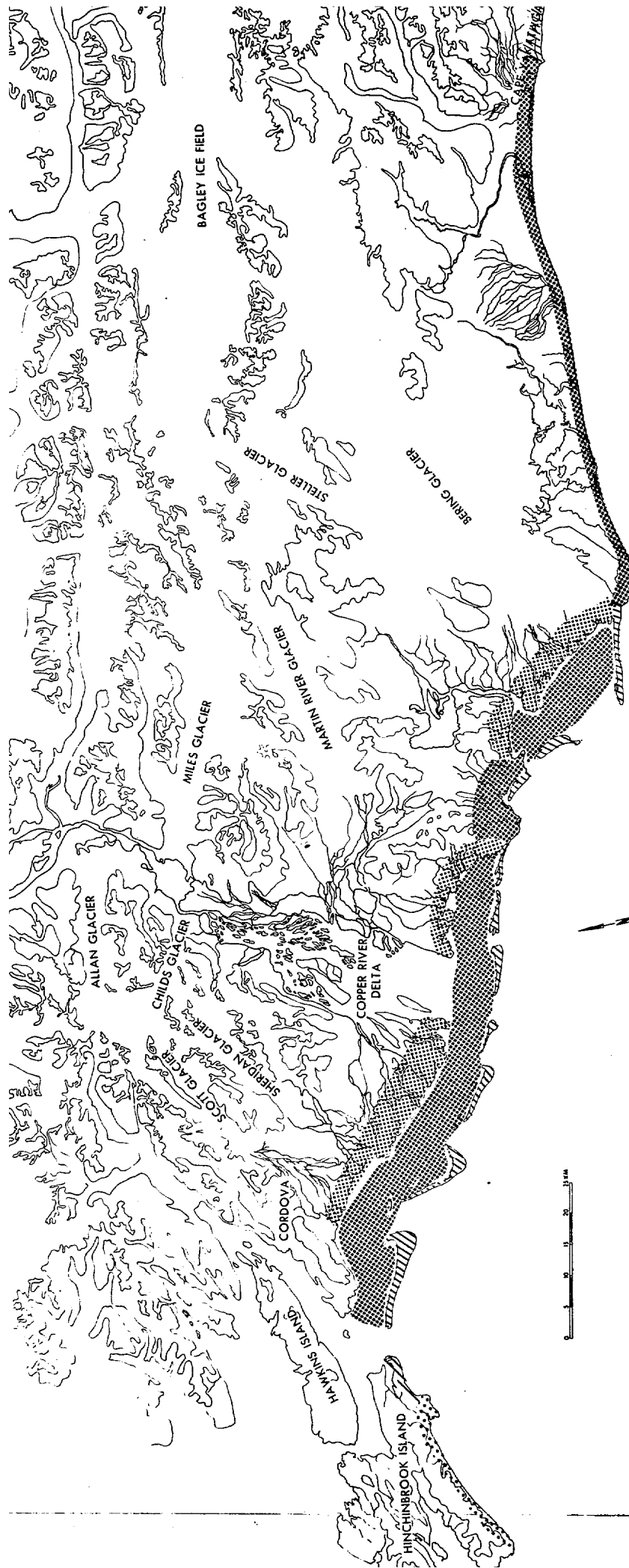
Included with this annual report is a set of topographic maps which have a color coded key to oil spill vulnerability. These maps are enclosed in a folder at the end of this report.

Figure 8. The following two pages display the Northern Gulf study area with the oil spill vulnerability risk classification. A set of topographic maps has been included with this report. The topographic maps utilize a color-coded key with considerably more **detail** than these black and white prints.

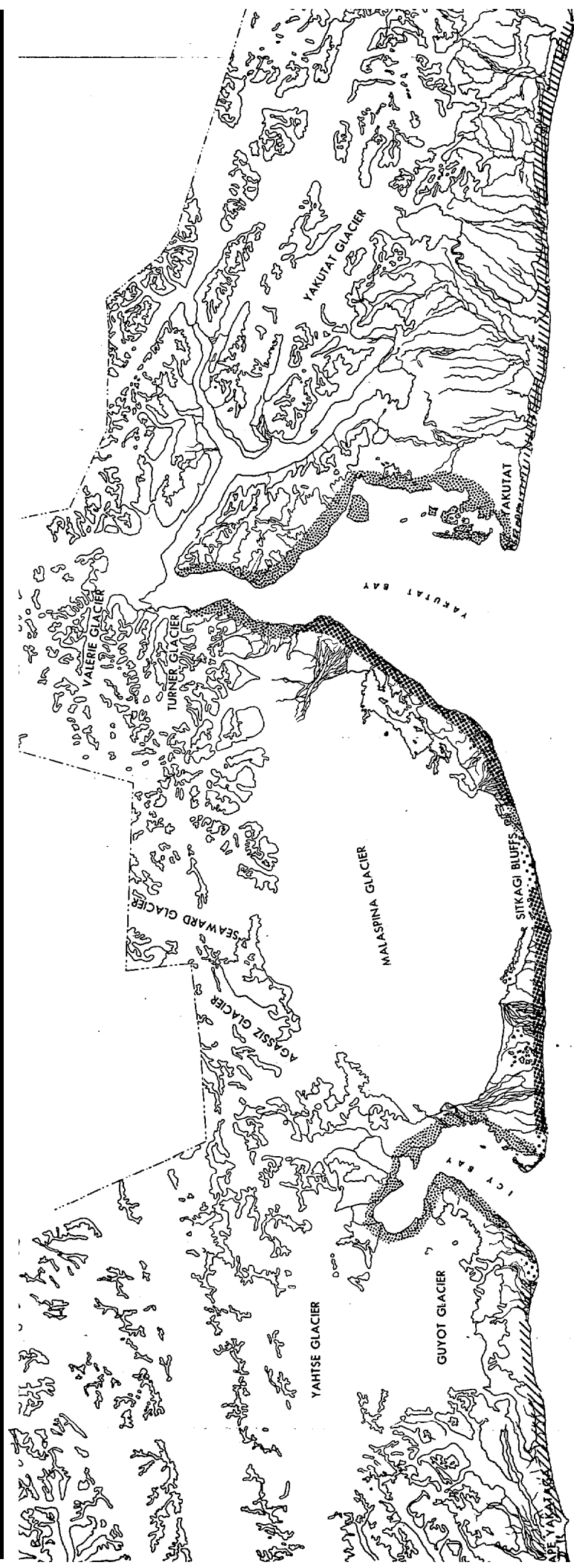
KEY TO FIGURE 8

OIL VULNERABILITY RISK CLASS

<u>RISK CLASS</u>	<u>OIL LONGEVITY</u>
 1-2	A few days to a few weeks.
 3-4	A month to six months.
 5-6	Less than 12 months.
 7-8	A year or two.
 9-10	Up to 10 years.



GULF OF ALASKA



GULF OF ALASKA



REFERENCES CITED

- Drapeau, G., Harrison, W., Bien, W., and Leinonen, P., 1974, Oil Slick fate in a region of strong tidal currents: **Proc. 14th Coastal Eng. Conf.**, p. 2245-2259.
- Drapeau, G., 1973, Natural cleaning of oil polluted seashores, **Proc. 13th Coastal Eng. Conf.**, Vancouver, B. C., p. 2557-2575.
- Harm, R. W., 1974, Oil pollution from the tanker Metula: Report to the U. S. Coast Guard, Texas A&M, **Civil Eng. Dept.**, 61 p.
- Hayes, M. O. and Gundlach, E. R., 1975, Coastal morphology and sedimentation of the Metula oil spill site in the Strait of Magellan: **Final Rept.**, Dept. Geology, U.S.C., 103 p.
- Hayes, M. O., Gundlach, E. R., and Perhac, R. M., 1976, The great Patagonian oil spill: Abstract, **AAPG-SEPM Annual Meeting**.
- Isakson, J. S., et al., 1975, Comparison of ecological impacts of postulated oil spills at selected Alaskan locations: USCG Rept. No. **CG-D-155-75**, V.1, 633 p., V.II, 865 p.
- Michel, J., Hayes, M. O., Brown, P. J., 1977, Application of an oil spill vulnerability index to the shoreline of lower Cook Inlet, Alaska, (i_n prep.).
- Owens, E. H., 1971, The restoration of beaches contaminated by oil in Chedabucto Bay, Nova Scotia, **Marine Sci. Branch**, Ottawa, Can., **Manus. Rep. Serv.**, No. 19, 75 p.
- Owens, E. H., 1973, The cleaning of gravel beaches polluted by oil, **Proc. 13th Coastal Eng. Conf.**, Vancouver, 33. C., p. 2543-2556.
- Owens, E. H., and Drapeau, G., 1973, Changes in beach profiles at Chedabucto Bay, Nova Scotia, following large scale removal of sediments, **Can. Jour. Earth Sci.**, 10, p. 1226-1232.
- Owens, E. H., and Rashid, M. A., 1976, Coastal environments and oil spill residues in Chedabucto Bay, Nova Scotia, **Can. Jour. Earth Sci.**, 13, p. 908-928.
- Rashid, M. A., 1974, Degradation of bunker C oil under different coastal environments of Chedabucto Bay, Nova Scotia: **Estuarine and Coastal Marine Sci.**, 2, p. 137-144.
- Robertson, B., Arhelger, S., Kinney, P. J., and Button, D. K., 1973, Hydrocarbon biodegradation in Alaskan waters: Center for Wetlands Resources, Louisiana State Univ., **LSU-SG-73-01**.
- Ruby, C. H., Fischer, F. A., Ward, L. G., Brown, P. J., 1977, Buzzards Bay oil spill - an Arctic analogue, Abstract, 4th Intern. Conf., Port and Ocean Eng. under Arctic conditions, Newfoundland, (in prep).

Ruby, C. H., and Gundlach, E. R., 1977, Ethyl H. oil spill in ice bound Hudson River, in prep.

Sartor, J. D. and Foget, C. R., 1971, Evaluation of selected earthmoving equipment for the restoration of oil contaminated beaches, Proc. Joint Conf. on Prevention and Control of Oil Spills, Wash., D. C., p. 505-522.

SEDIMENTOLOGY

Christopher H. Ruby

Sampling Technique and Method of Analysis

Sediment samples were collected at each of the DBC profile sites (Fig. 1) and at each of the permanent profile sites (Fig. 2). The sampling plan illustrated in Figure 3 was used. In all cases, at least 3 samples were taken, using a 15 cm coring tube. Where dunes were present behind the beach, a "D" sample was taken. In addition, sediments with unusual composition or texture were also sampled and are labeled with an X, Y, or Z (see Appendix, Table 1). Finally, where the grain size of the sediments present was too large to collect a representative sample, photographs were taken and later analyzed using a projector.

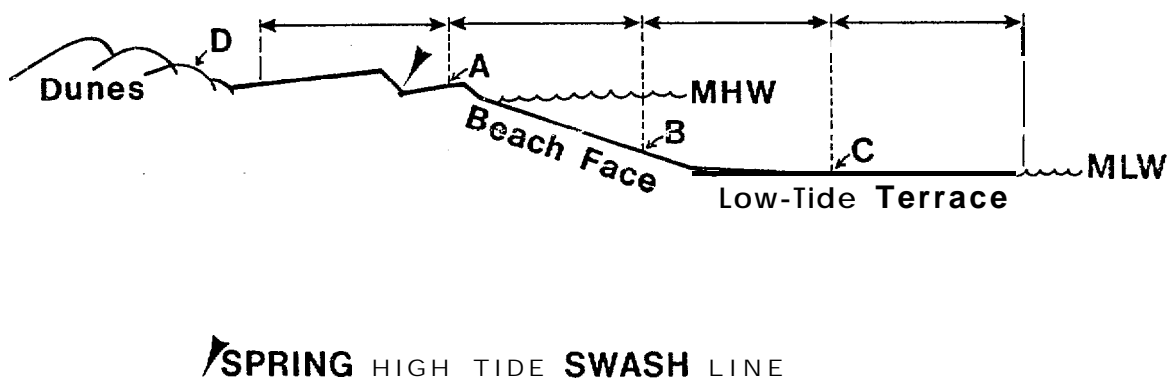


Fig. 3. Beach zone sampling plan. Samples A, B, and C are taken from the upper, mid, and lower beach face, respectively. Sample D is taken from any dunes present behind the beach face. All samples are 15 cm cores.

All sediment samples were analyzed for grain size parameters using a Ro-Tap machine and sieves at $\frac{1}{4} \phi$ intervals. Grain size parameters were then computed

¹The symbol ϕ designates units (ϕ units) used in grain size conversions (from mm) for ease of statistical computation. The ϕ scale, devised by Krumbein (1934), is a logarithmic transformation of the Wentworth size scale that is based on a constant ratio of 2 between classes. Hence, the following relationships exist:

ϕ	mm	sediment type
-4.0	16	pebble
-1.0	2.0	boundary between sand and gravel
+1.5	0.35	medium sand
+4.0	0.0625	boundary between sand and silt
+6.0	0.0156	medium silt

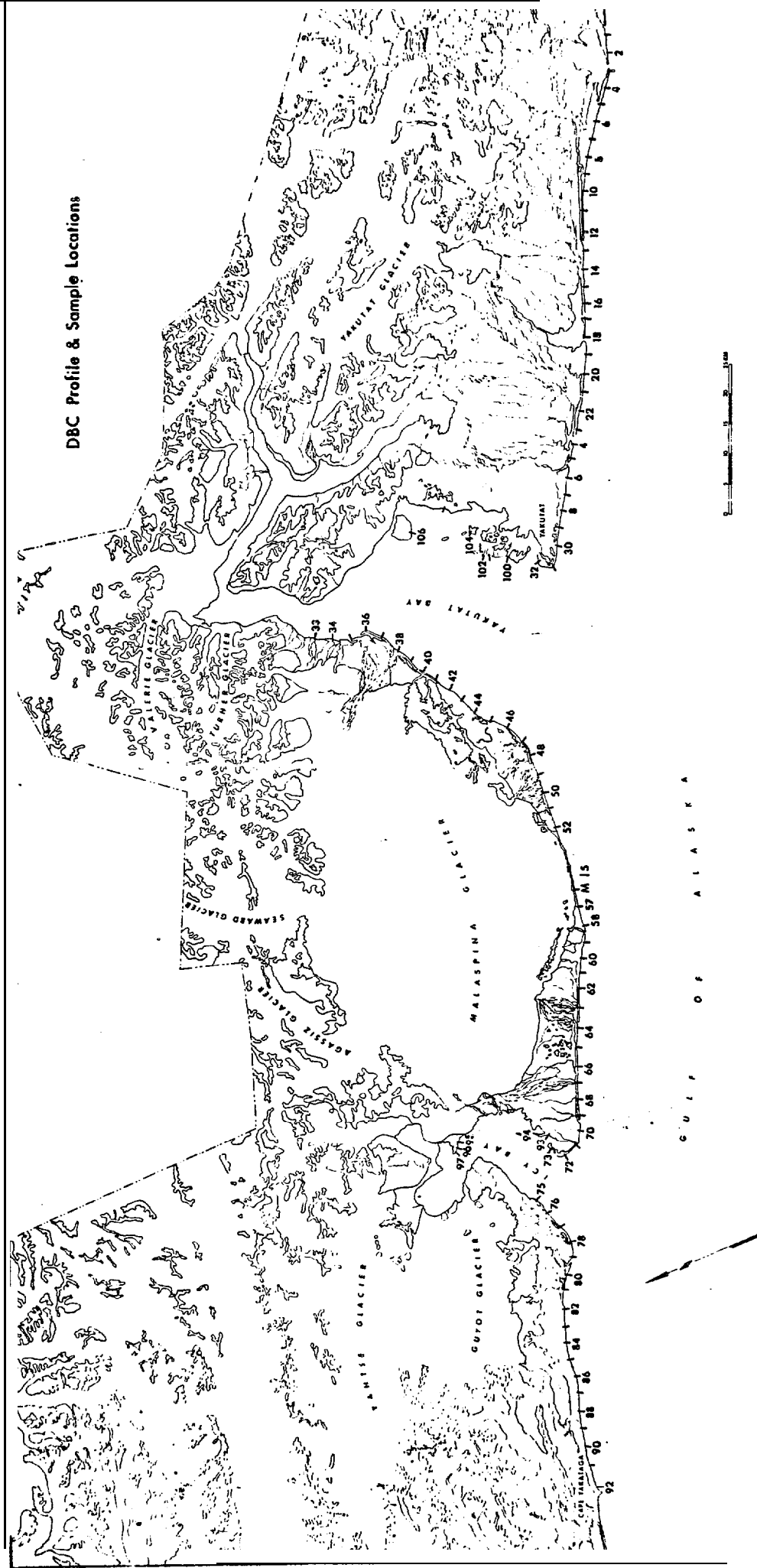


Figure 1. DBC sample sites in the Northern Gulf of Alaska

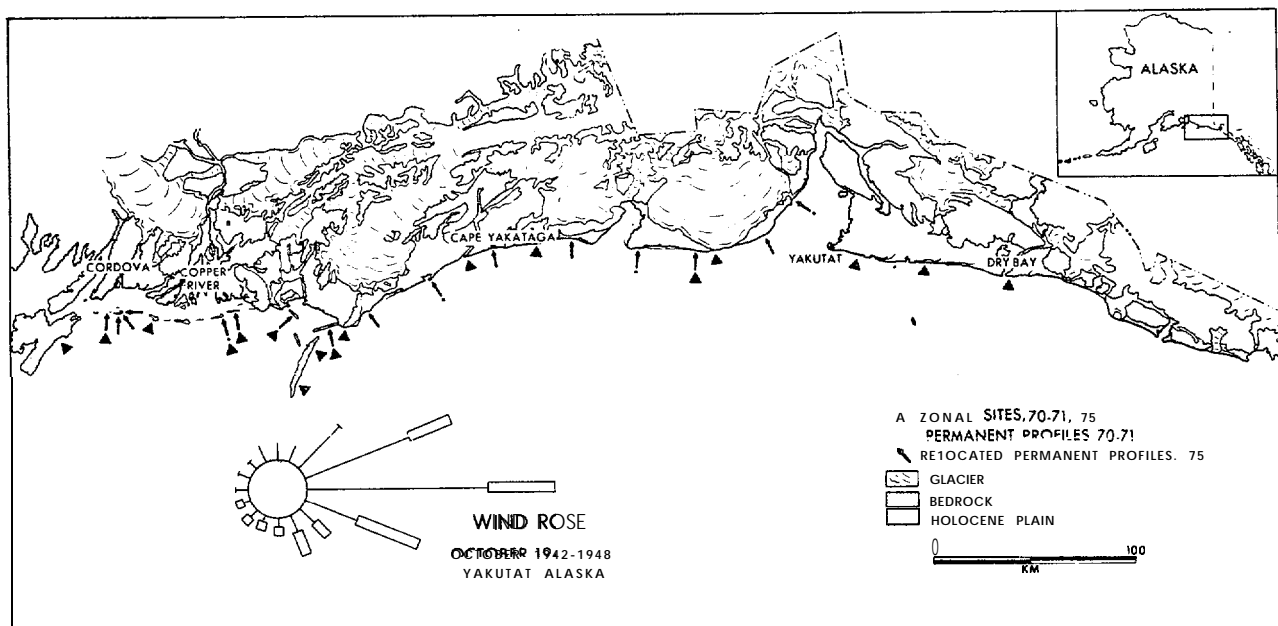


Figure 2. Permanent profile sampling sites in the Northern Gulf of Alaska.

by the method described by Folk (1968). They are as follows:

Graphic mean (Mz)	$\frac{\phi 16 + \phi 50 + \phi 84}{3}$
Inclusive graphic standard deviation	$(\sigma_I) \frac{\phi 84 - \phi 16}{4} + \frac{\phi 95 - \phi 5}{6.6}$
Inclusive graphic skewness (a measure of symmetry of of the grain size distribu- tion)	$\frac{\phi 16 + \phi 84 - 2(\phi 50)}{2(\phi 84 - \phi 16)} + \frac{\phi 5 + \phi 95 - 2(\phi 50)}{2(\phi 95 - \phi 5)}$

The results were synthesized by computer. Mean grain size, standard deviation and skewness for each of the samples is given in Table 1 in the Appendix. Complete sediment data are available on magnetic tapes from NODC (see reference list).

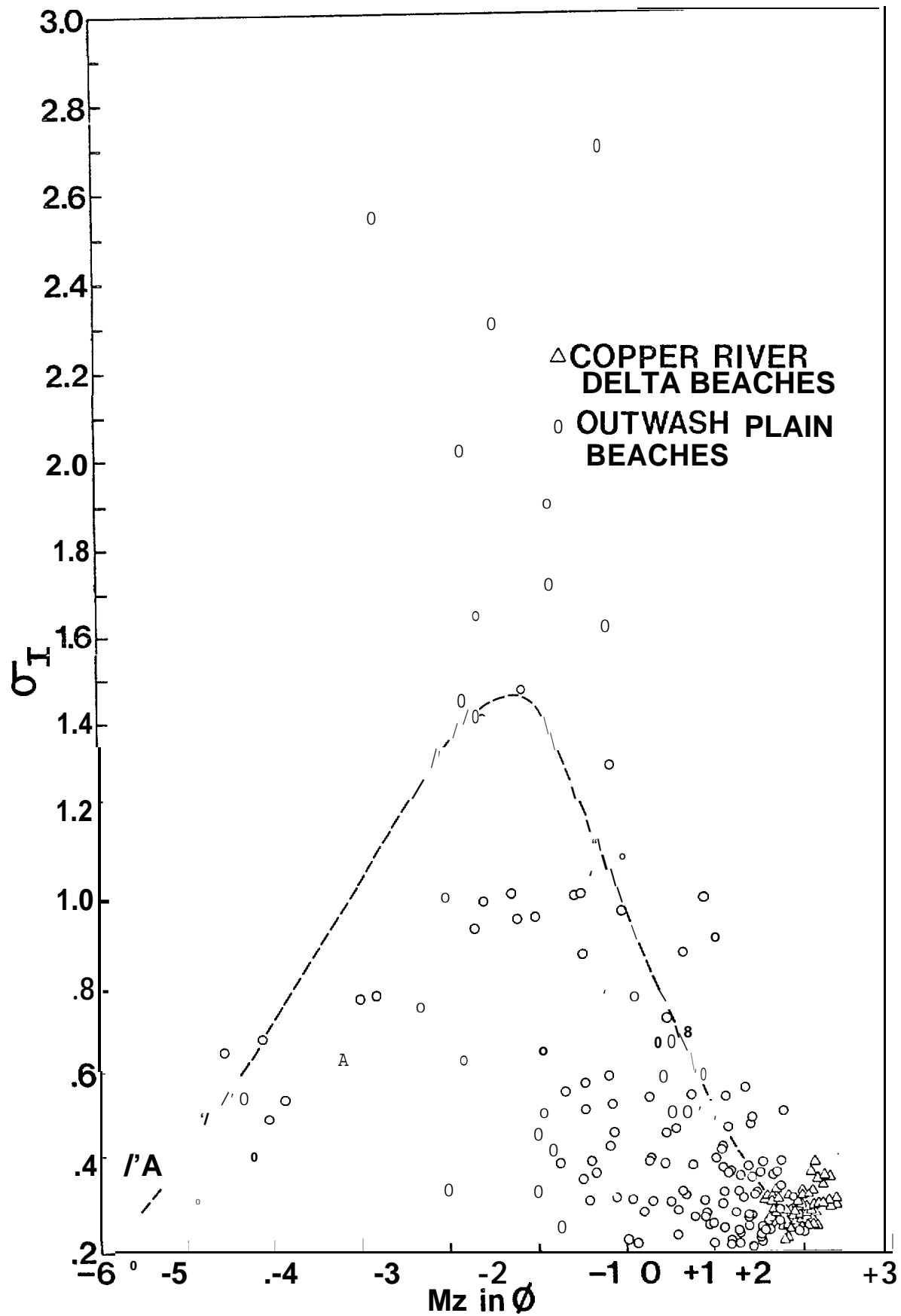
TEXTURE

Introduction

The sediments of the study area vary over an extremely wide grain size range, from large glacial erratics, 10's of m in diameter, left behind by retreating glaciers, to silts and clays on tidal flats and marshes. Most of the beaches, however, are composed of mixes of sand and gravel. Sorting, therefore, is usually poor.

1969-1970 Data. - Using the samples collected during the 1969-1970 field seasons, a comparison of the beach sediments of the Copper River delta vs. beaches bordering outwash plains has been made. Figure 4 shows the result of this comparison. Note that the Copper River delta beach sediments are finer and better sorted than those of the beaches bordering outwash streams. Compositional analysis (Fig. 5) indicates a higher percentage of quartz in the Copper River delta beach sediments, although they still plot as litharenites in Folk's (1974) classification (Fig. 6). Thus, the Copper River delta beach sediments are considerably more mature, both texturally and compositionally, than the sediments of the beaches bordering outwash streams. The poorest sorting occurs in sediments with a mean grain size between the 0φ and -2φ (Fig. 4). That size is at the midpoint between the two pri-

Figure 4. Graph of grain size vs. standard deviation (sorting) for sediment samples collected during 1969-1970 field seasons. Note inverted "V" distribution explained in the text. Also note the finer better sorted nature of the sediments from the Copper River delta beaches.



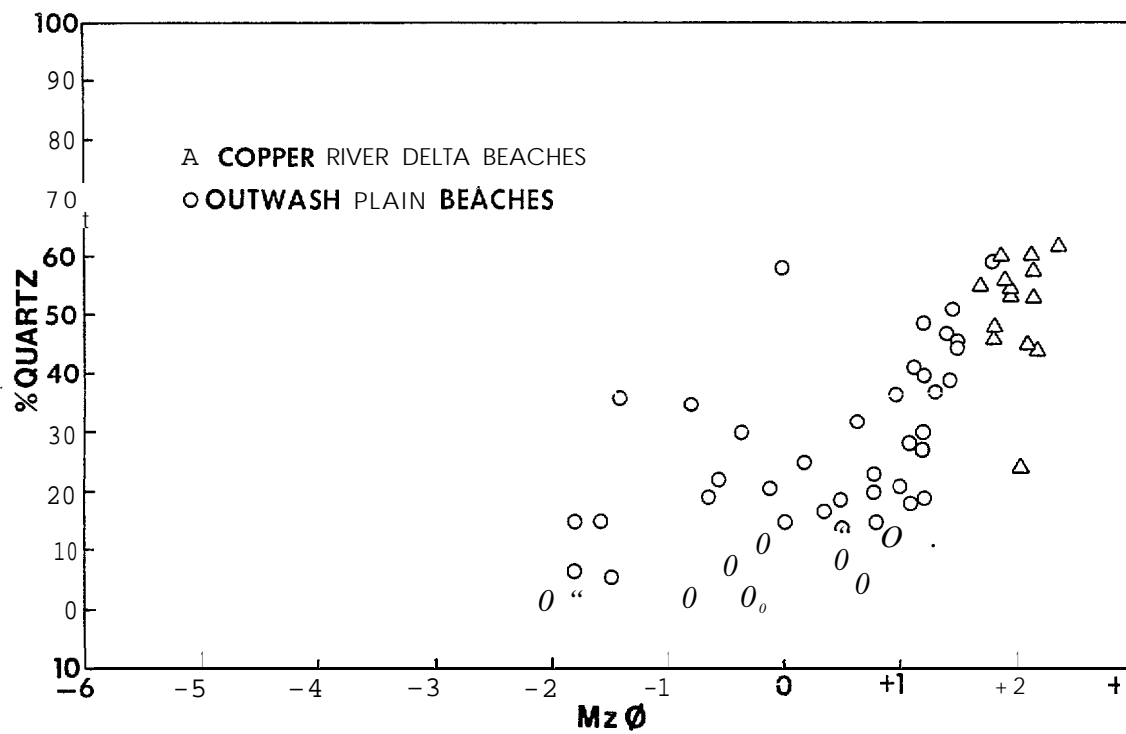


Figure 5. Graph of % quartz vs. grain size for 1969-1970 sediment samples. Note the high quartz % and fine texture of the Copper River delta sediments.

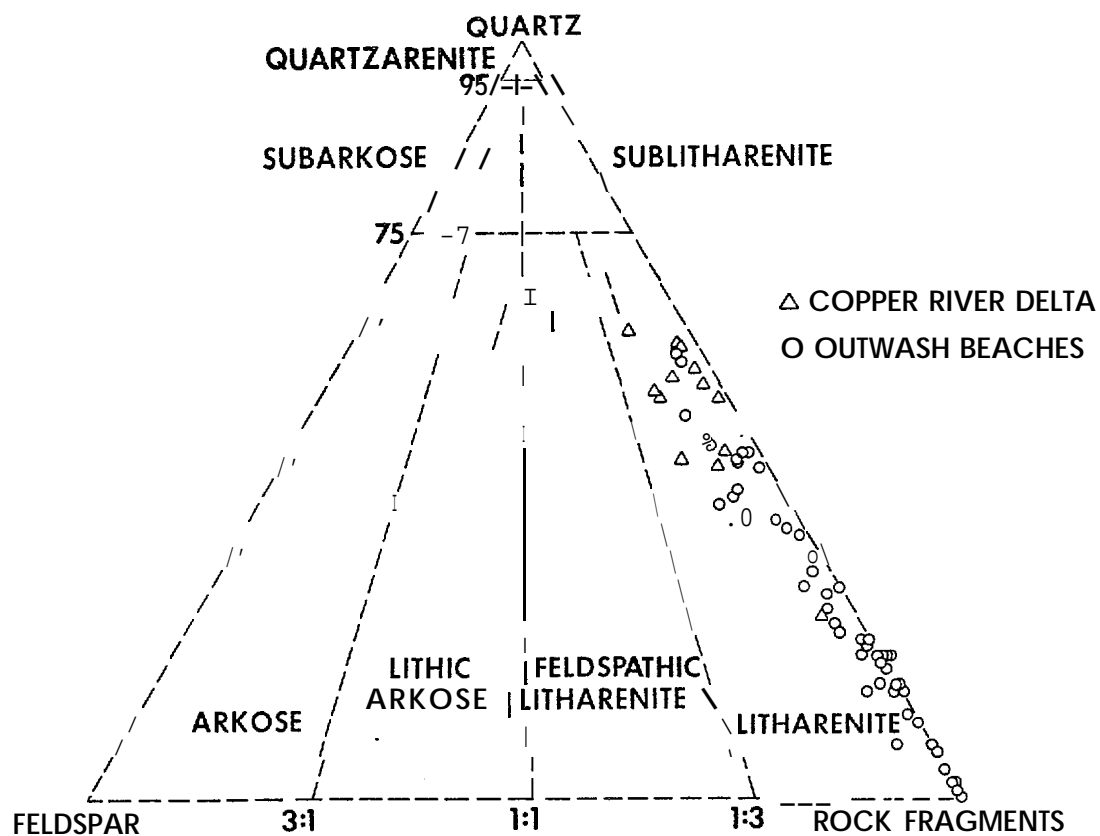


Figure 6. Compositional diagram of the 1969-1970 sediments of the Copper River delta as more quartz rich but still plot as litharenites.

mary grain size modes (sand and gravel) of the sediments of the area. Decreasing the grain size (moving to the right on the diagram) (Fig.4) results in a loss of the coarse mode and thus better sorting. Increasing the grain size (moving to the left on the diagram), results in a loss of the fine mode and thus better sorting. This natural mixing at two modal sizes is a common occurrence and has been well documented in the literature (Folk and Ward, 1957; Folk, 1968). Thus, the inverted "V" distribution shown in Figure 4 conforms with these concepts and should not be considered unusual,

1975 Data (Yakutat Foreland). - During the 1975 field season, over 400 sediment samples were collected at the DBC sites and at the permanent profile sites. The 3 km spacing of the DBC sites permits a more detailed analysis of grain-size parameter changes along the beaches of the study area. Numerous trends are evident.

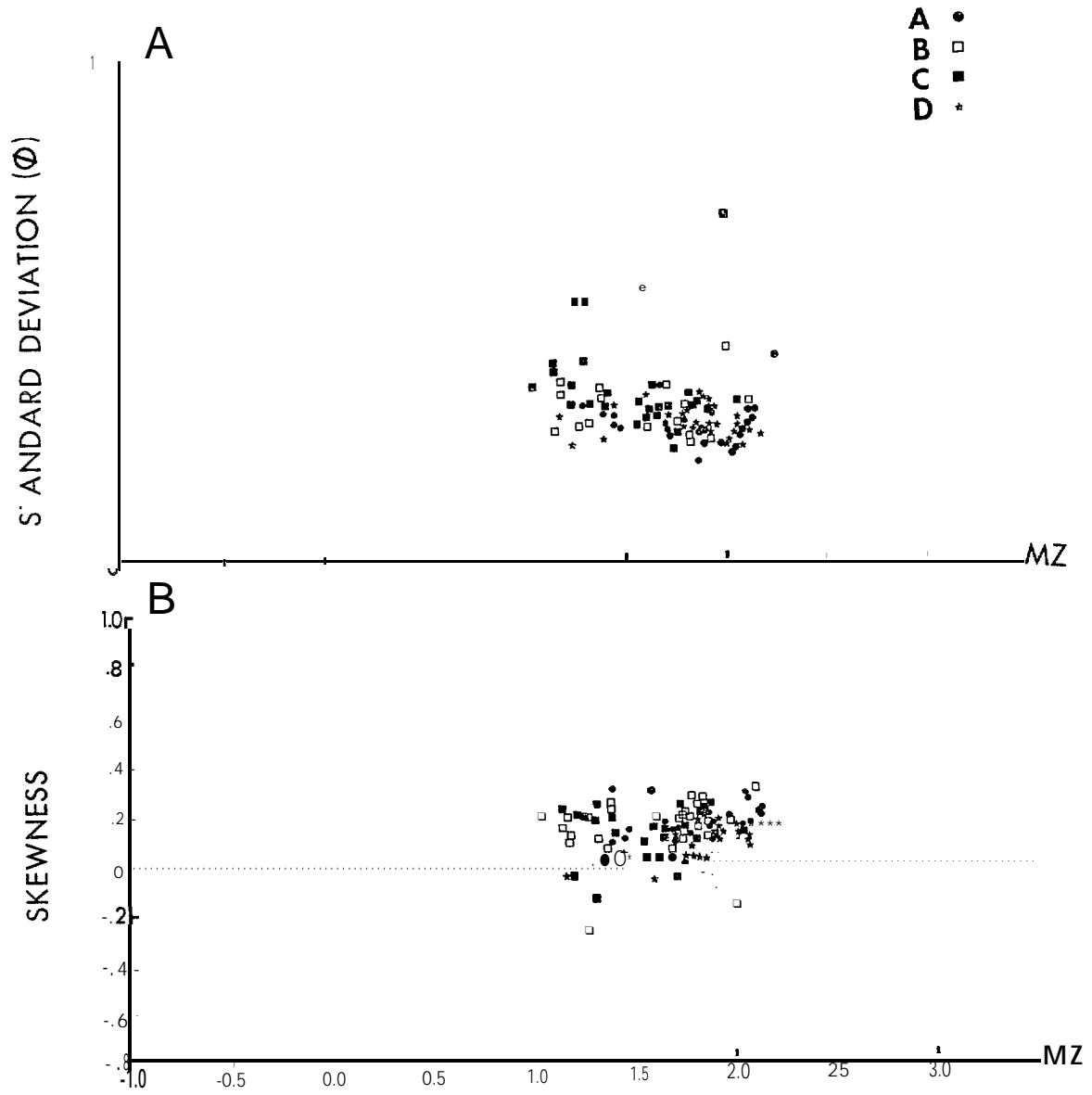
The 90 km stretch of coast from Dry Bay (DBC-3) to Yakutat Bay (DBC-32) demonstrates some of these trends. A 25-km wide outwash plain, called the Yakutat Foreland, was formed by outwash streams that drained numerous glaciers in the St. Elias Mountains in early to middle Holocene times. The present outwash streams must flow across 25 km of relatively flat topography before reaching the Gulf of Alaska. Much of the coarse sediment transported by these streams is deposited close to their glacial sources. The sediment that does reach the coast, is considerably more mature than it would otherwise have been if the stream sources were close to the coast, as they are on the Malaspina Foreland. Additionally, many of these streams emanate from glacial margin lakes which act as sediment traps. This geomorphic setting results in the supply of relatively fine sediments to the coast. The sediments carried by these rivers at their mouths are primarily sands.

The grain size parameters of the beach sediments of the Yakutat Foreland are graphically represented in Figure 7. Part A shows the relationship between mean grain size and sorting (standard deviation σ_I). The sediments cluster between $+1\phi$ and $+2\phi$ (medium to fine sand) and generally are relatively well sorted. Part B

Figure 7 A. Graph of grain size vs. standard deviation (sorting) of sediment samples from the Uakutat Foreland. Note the highly clustered nature of the sediments between the 1.0 and 2.0 ϕ size interval.

Figure 7 B. Graph of grain size vs. skewness for the sediments from the Yakutat Foreland. The samples are generally positively skewed.

DBC 3 through 32



shows the relationship between mean grain size and skewness. The samples are generally positively skewed, indicating the presence of a finer minor size mode. Thus, the sediments in this stretch of coast are relatively mature with regard to grain size parameters. This tends to support the statements made above regarding the outwash stream length.

In order to test a hypothesis that most of the sediment supplied to this area is derived from the Alsek River, which empties into Dry Bay, grain size parameters were graphed against increasing distance downdrift (west) of Dry Bay. Since drift is to the west, we would expect a maturing of sediments in that direction. Figure 8 shows the relationship between the mean grain size of each A, B, C, and D sample with increasing distance from Dry Bay. There is a general reduction in grain size along this 90 km shoreline. Sample A is consistently finer than either B or C samples. The A sample is taken from high on the beach face at about the location of the storm berm. As can be seen in Figure 8, the A and D samples are similar in size, both being finer than the B and C samples taken from the mid and lower beach face respectively.

The considerable scatter evident in Fig. 8 made it difficult to determine what was taking place at the numerous river inlets on this shoreline. In order to get a clearer picture of grain size variation across these inlets, the cumulative frequency graphs (plotted by computer) were analyzed for grain size modes. Major modes were defined as those containing 10% or more of the distribution. Minor modes were picked out visually from the curves. The results of this modal analysis are given in Table 2 in the Appendix. Figure 9 shows the relationship of the grain size of the major modes versus distance from Dry Bay. Since the modes were defined at 1% intervals, there is less scatter in the distribution. Note that A and D samples are again finer than B and C samples. Also, there is considerable stability in the modal grain size of the B sample over distance. By following the B sample, one can see that most of the variation occurs at the inlets. There is a prominent fining across the Akwe River inlet, indicating that it is acting as a supplier of

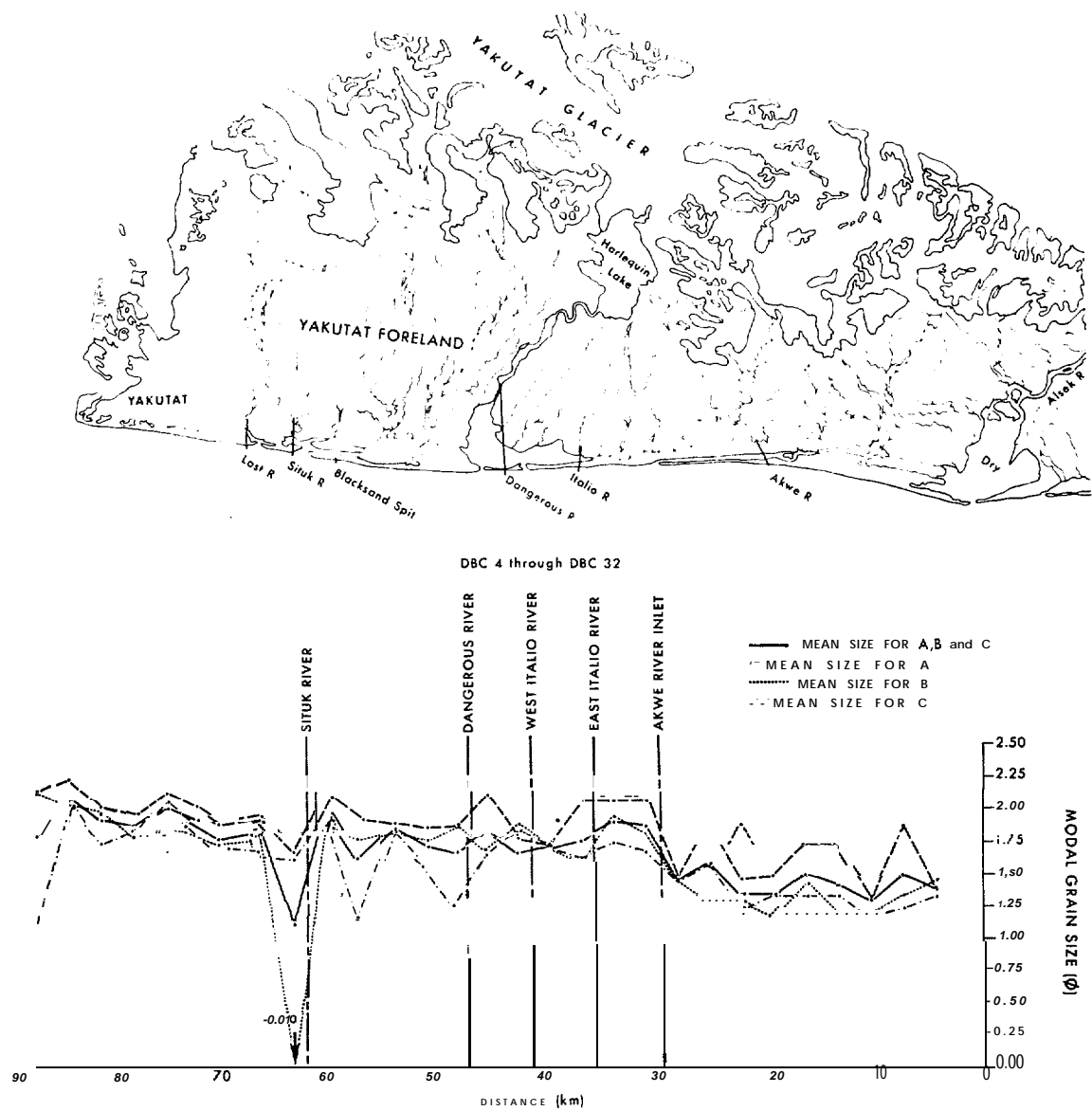


Figure 8. Graph of the mean grain size of Yakutat Foreland samples vs. distance downdrift of Dry Bay. Note that the sediments fine in the downdrift direction.

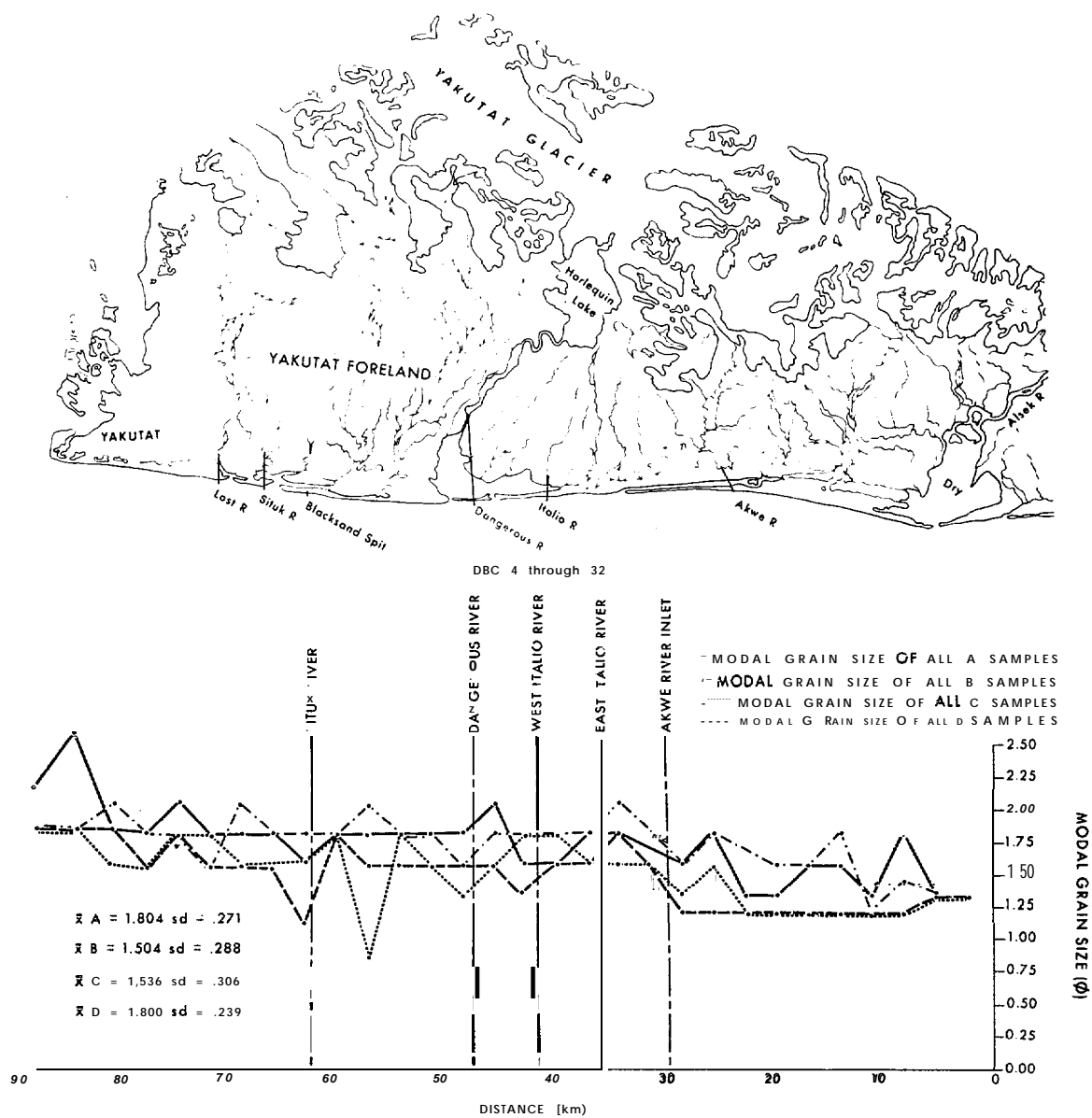


Figure 9. Graph of modal grain size of Yakutat Foreland samples vs. distance downdrift of Dry Bay. Samples show a fining tendency in the downdrift direction.

fine sediment ~~or~~ as a sorting mechanism to eliminate more coarse sediments. Each of the other inlets demonstrate a fine updrift side and a coarser downdrift side, indicating the input of a minor coarse mode. With this in mind, **it would** seem likely that the Akwe River inlet is sorting out the finer sediments from updrift rather than introducing them itself. This would agree with studies at tidal inlets done by Winkelmoen and Veestra (1974). Here again, the overall picture is a gradual reduction in grain size from Dry Bay to Yakutat Bay, with the B sample being a more stable indicator than the others.

We have considered taking only one beach face sample on future field studies; thus, we wanted to test the B sample to see how it represented the grain size range on the beaches. Figure 10 shows the modal grain size of the B samples compared to the mean of the modal grain sizes of A, C and D samples. The B sample is generally about 0.2~~0~~ coarser than the mean of the A, C and D samples. This is primarily the result of the fine nature of the A and D samples. **It** follows rather closely the trend of the A, Canal D samples and is considered to be the best single sample to use for this type of study.

Finally, a comparison of the D sample taken from dunes located behind the beach face was made with the A, B and C samples taken from the active beach face. Figure 11 shows the result of comparing the major modal grain size of D samples with the mean of the major modal grain size of the A, B and C samples. It is clearly evident that the beach sediments are coarser than the dune sands. This is a well known phenomenon.

Sorting has been used previously by the Coastal Research Division to delineate transport trends (Nummedal et al., 1974). Figure 12 displays the sorting of the A, B, C and D samples graphed against distance from Dry Bay. Unfortunately, no clear trend is evident from this graph. Calculating the mean sorting of A, B, C and D samples taken together and then plotting that on the same X axis, Figure 13 still shows no clear trend from Dry Bay to Yakutat Bay. However, the graph does **show** an interesting tendency for the sediments to be more poorly sorted on the

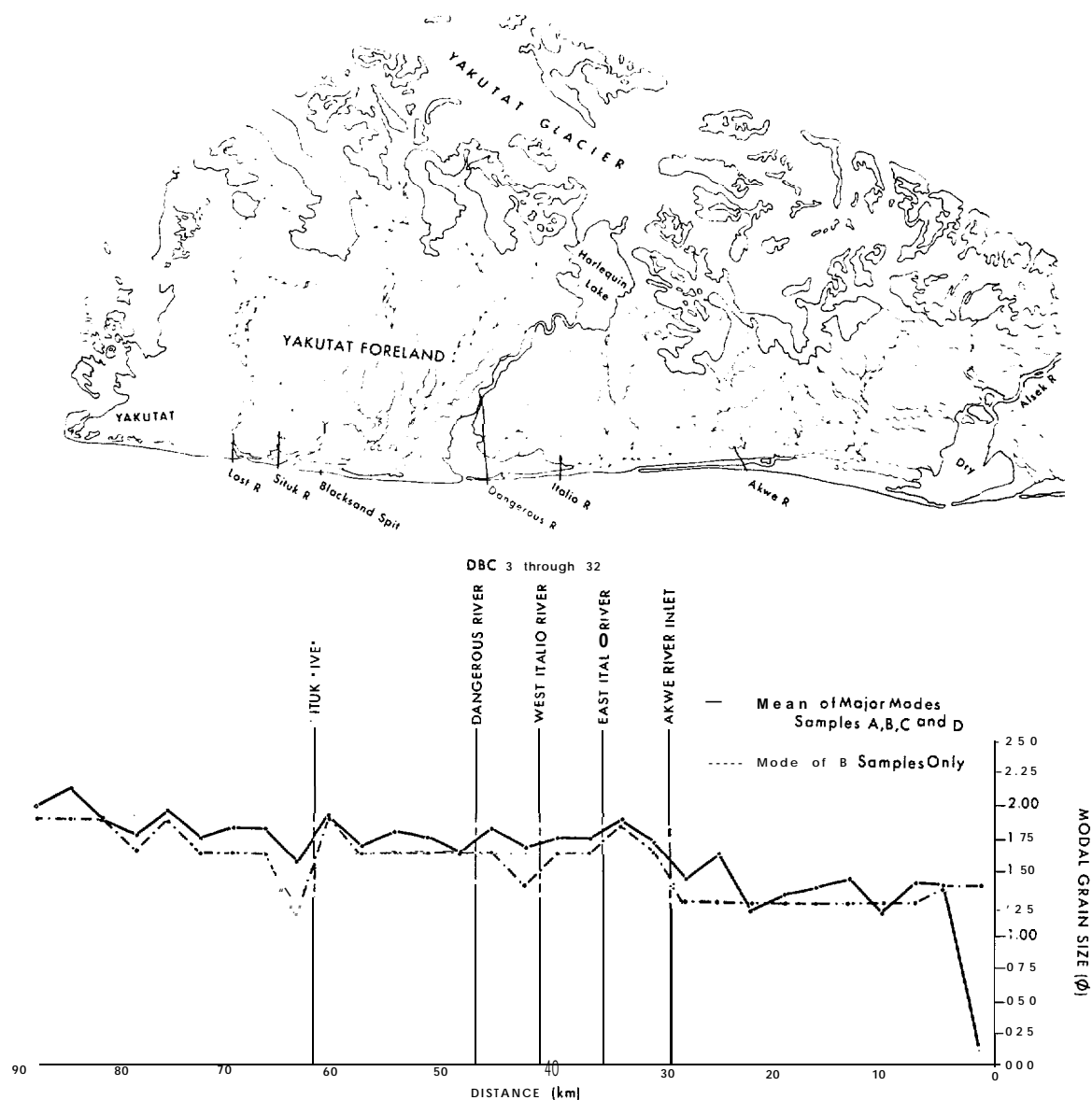


Figure 10. Graph of the modal grain size of "B" samples , and the mean of the modal grain sizes of A, C, and D samples vs. distance downdrift of Dry Bay. The "B" sample is generally slightly finer than the mean of the A, C and D samples. It is also a more stable indicator.

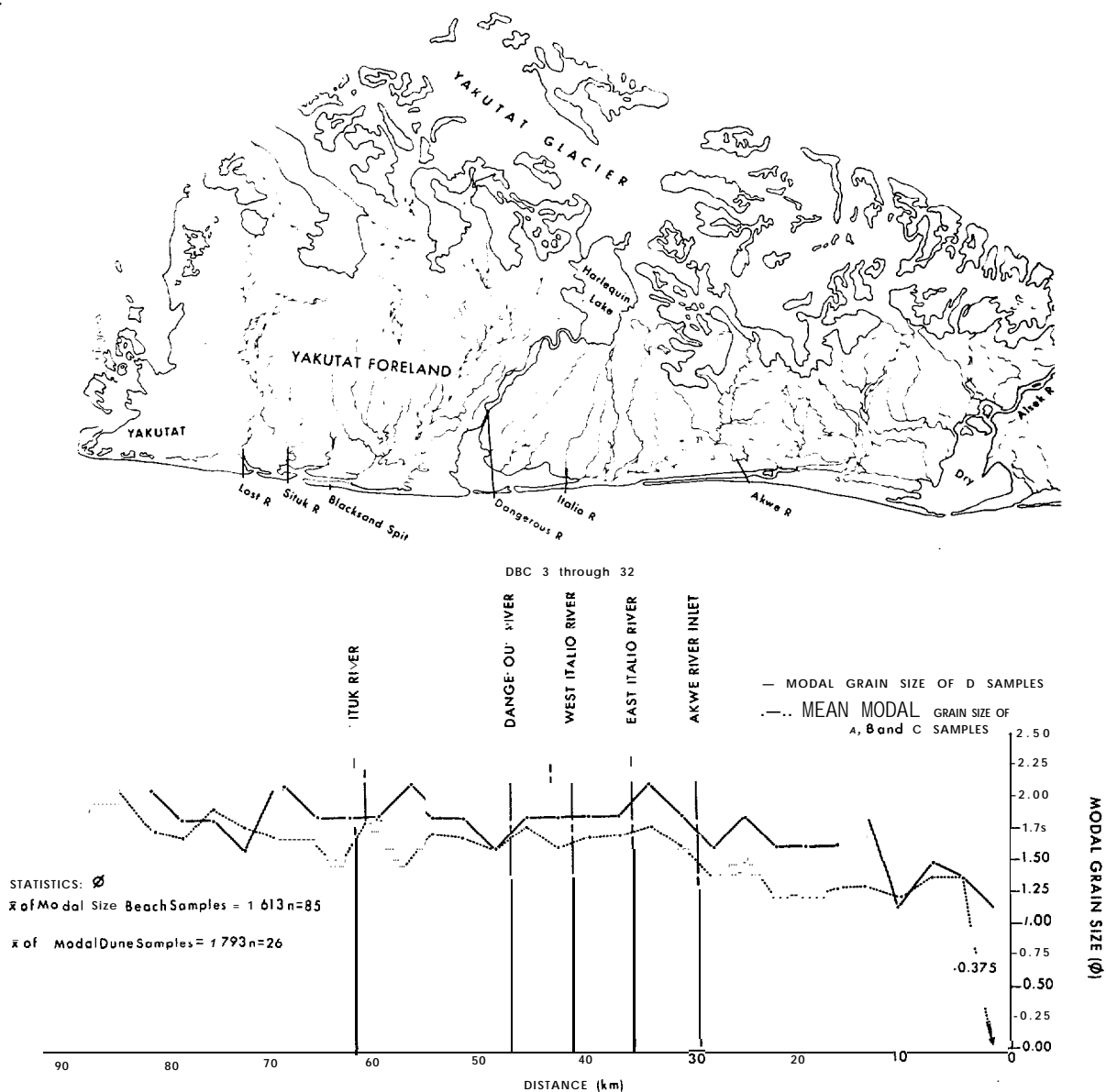


Figure 11. Graph of modal grain size of. "D" samples and the mean of the modal grain size of A, B, and C samples vs. distance downdrift of Dry Bay. The "D" sample is consistently finer than the A, B, and C sample means.

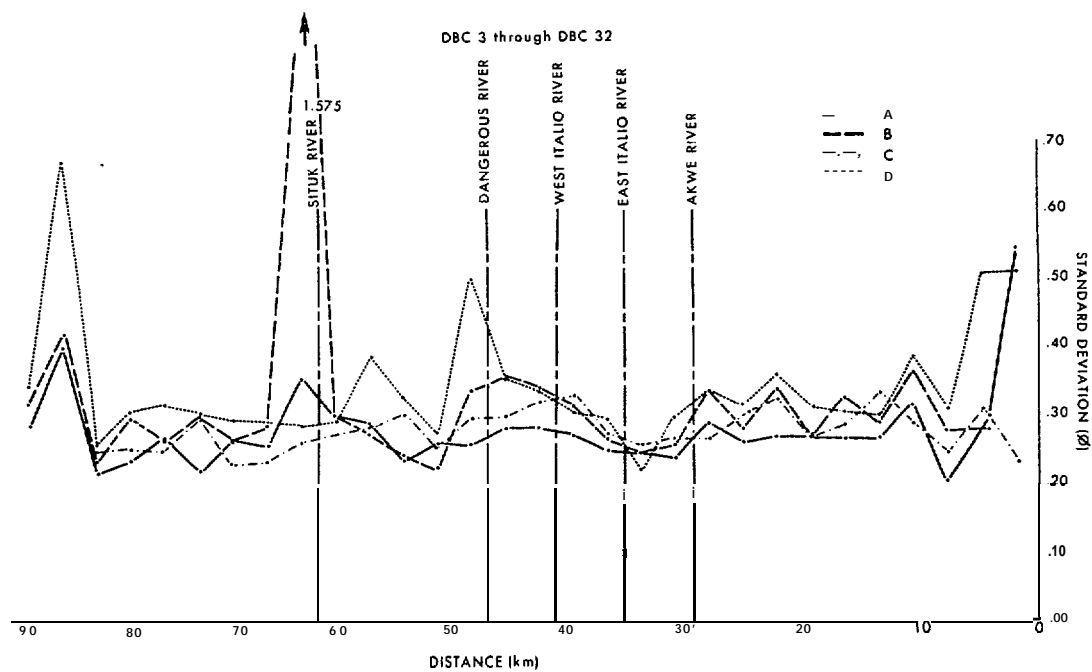
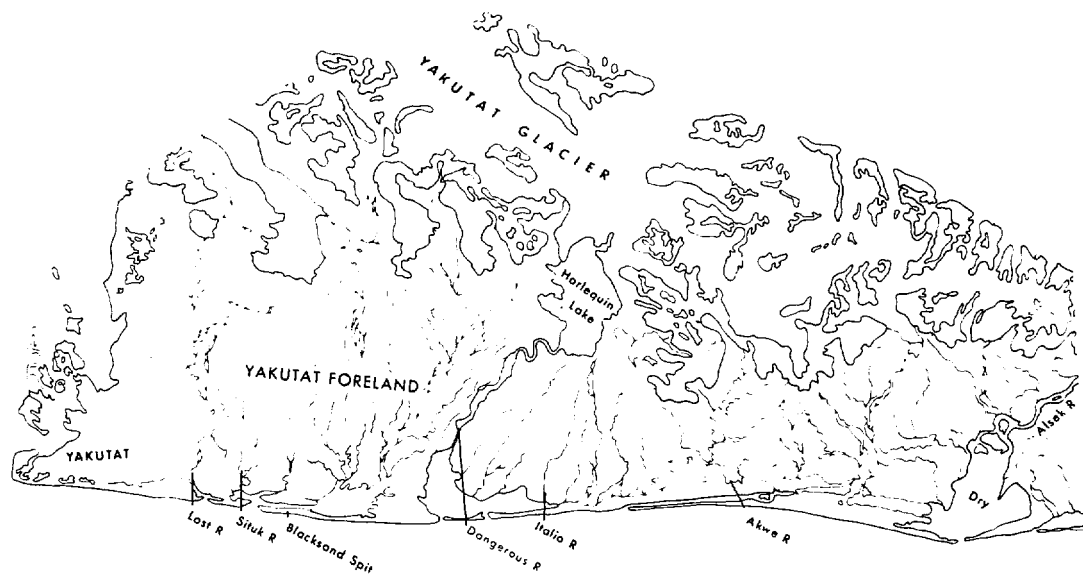


Figure 12. Graph of the standard deviation (sorting) of the Yakutat Foreland samples vs. distance downdrift of Dry Bay. No clear trend is evident; however, most variation occurs at river inlets.

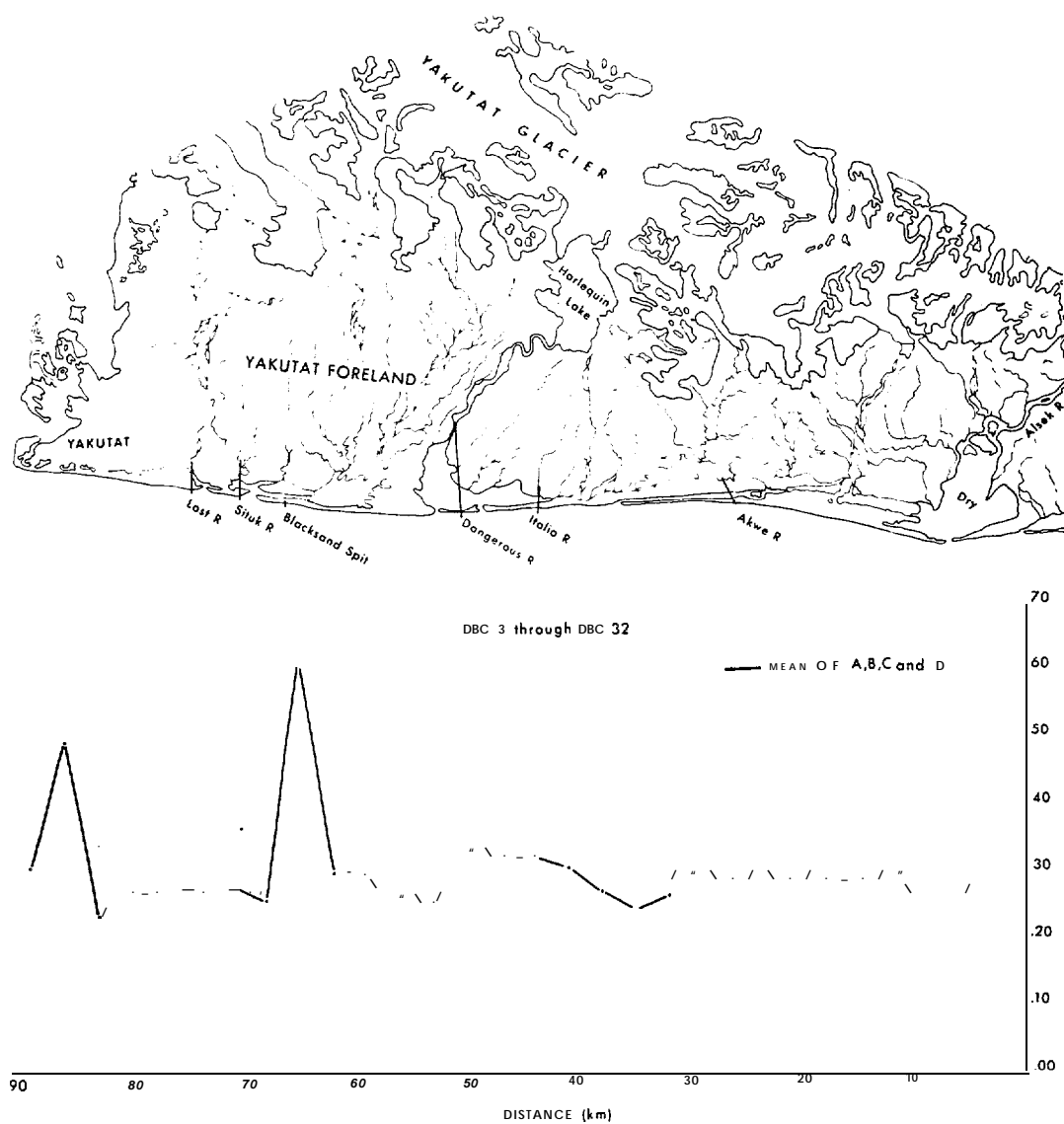


Figure 13. Graph of the mean sorting of A, B, C and D samples vs. distance downdrift of Dry Bay. No clear trend is evident.

downdrift side of the river inlets. This tends to support the hypothesis that the rivers are transporting a slightly coarser minor grain size mode, discussed earlier in this section.

In summary, grain size parameters can be used to delineate sediment transport trends. Even on a coastline, such as the one between Dry Bay and Yakutat Bay, interrupted by numerous rivers, classic concepts relating to sediment maturing can be detailed with careful laboratory analysis of the sediments.

1975 Data (Yana River to Riou Spit). - A second section of shoreline, between the Yana River Spit and Riou Spit in Icy Bay (Fig. 1) was selected to do a visual grain size analysis. This 32 km shoreline was divided into 32 sample sites located at a one km interval. At each site, the active beach face was subdivided into 8 equal sections, and a sample was taken from the center of each section. Thus, a total of 256 samples were analyzed, using a $\frac{1}{40}$ interval hand-held visual size estimator. Sorting, gravel size, and % gravel were also analyzed visually for each sample. Figure 14 graphically displays some of the results of that study. The sections at the top, bottom, and midpoint of the beach were selected for this graph. The mean of the three samples has been used in the plots. A number of trends are evident.

The inflection point on Riou Spit (where it turns 90° into Icy Bay) is acting as a sediment sorting locus. Note that the sand grain size at that point is the coarsest on the graph. Also, the % gravel is high, although the relative gravel grain size (calculated visually on a scale from 1 to 7 ranging from granule to cobbles) is rather fine. From that point to the end of the spit (downdrift), the sand size decreases, as does the % gravel. This conforms to the general rule of sediment fining in the direction of dominant sediment transport. The gravel grain size increases, however, due to a glacial platform underlying the spit near its downdrift end. This glacial till platform has formed a boulder and cobble low-tide terrace over which the spit is prograding. Thus, the inflection point is acting to sort out coarser grain sizes (gravels and coarse sands) while bypassing

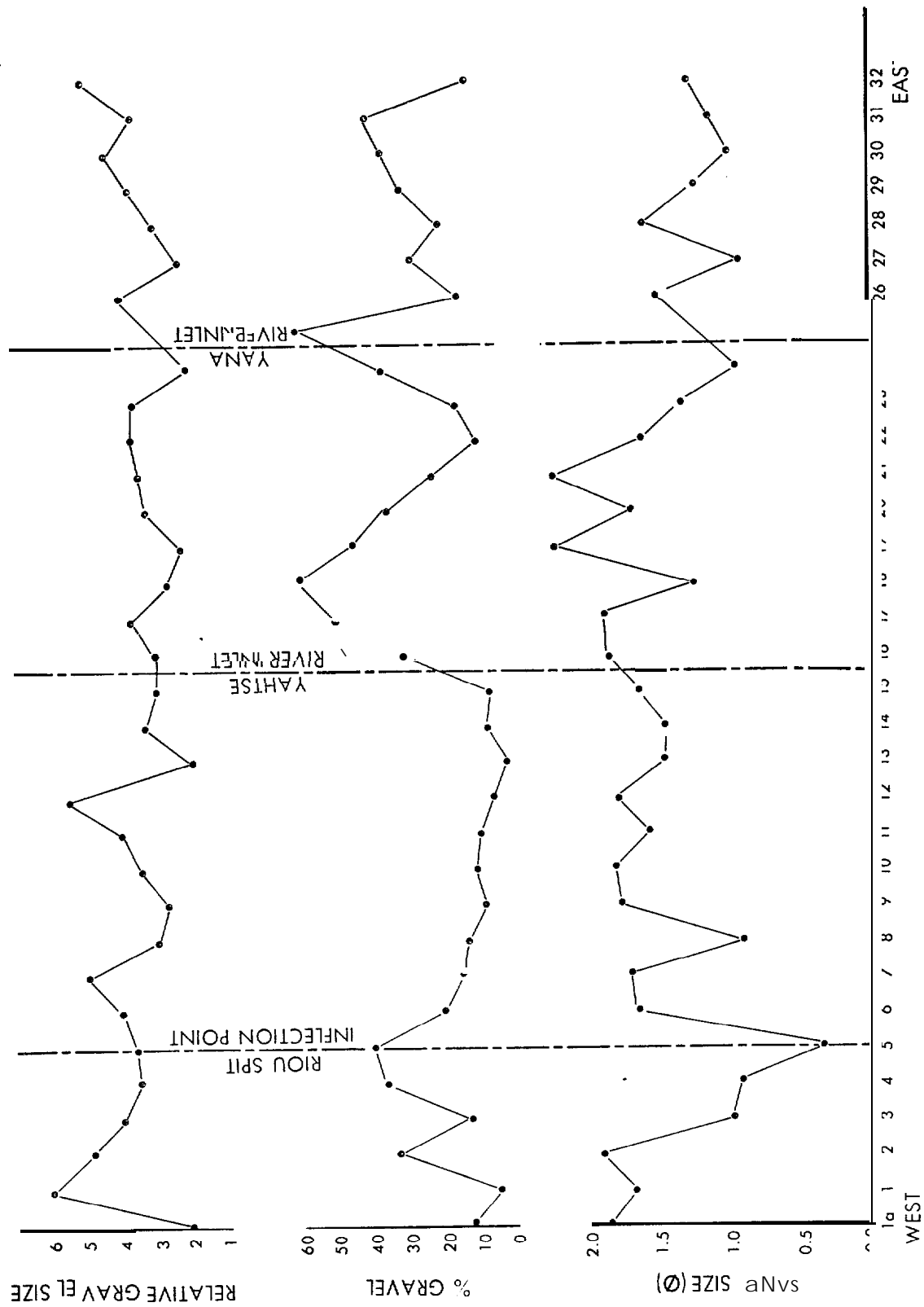


Figure 14. The parameters of sand grain size, % gravel, and relative gravel grain size are graphed vs. distance on the West Malaspina Foreland. Stations on the "X" axis are 1 km apart. Trends are explained in the text.

the finer sediments. At the inflection point, the spit is prograding into deeper water (Nummedal and Stephen, 1976). Much of the sediment moving along the spit is deposited here, including the vast majority of the coarser sediments. However, the progradation of this particular portion of the Riou Spit acts to shelter the glacial platform behind it. This sheltering results in considerably smaller waves which are, therefore, only capable of carrying the finer sediments. Thus, the spit is also prograding into the bay, over the platform, by the addition of fine sand.

Another trend, evident from Figure 14, is a pronounced deposition of gravels at the updrift (east) side of the river inlets. In conjunction with this trend is a coarsening of the sand grain size from the updrift to the downdrift side of the inlets. This agrees with the trends on the Yakutat Foreland.

Finally, the means of the grain size parameters for each section from the top to the bottom of the beach were calculated. Figure 15 shows that the % gravel increases as the toe of the beach is approached. This is the result of the increased exposure of the lower parts of the beach face to wave action. Relatively large waves are required to move the gravels. Thus, most of the gravel is moving at the base of the beach while the sand fraction is moving throughout the beach face. The sand size graph in Figure 15 also shows a sharp increase in sand size at the base of the beach face, probably the result of the same process.

1975 Data (Malaspina Foreland). - A final grain size trend analysis was done on the Malaspina Foreland. This area is dominated by the Malaspina Glacier, which is drained by a number of very active glacial outwash streams with sources close to the shoreline. It contrasts well with the Yakutat Foreland. Fifteen sites were sampled either visually (for very coarse sediments) or using standard sieving techniques. Figure 16 graphically displays the results of this analysis. The graph shows the mean of A, B, and C samples taken at the 15 sites in 1970 (Hayes et al., 1970). It is immediately obvious that there is a fining of sediments both to the east and to the west of Sitkagi Bluffs. In their earlier report,

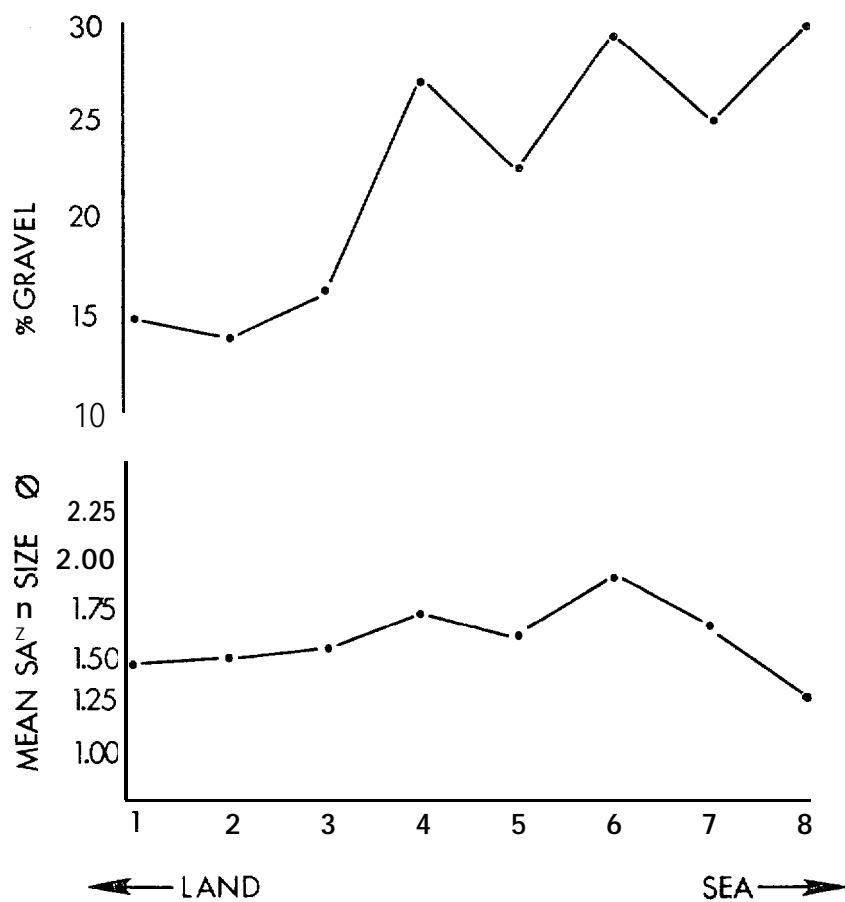


Figure 15. Graph of % gravel and sand size vs. position of beach face. Gravel % increases and sand size increases as the toe of the beach is approached.

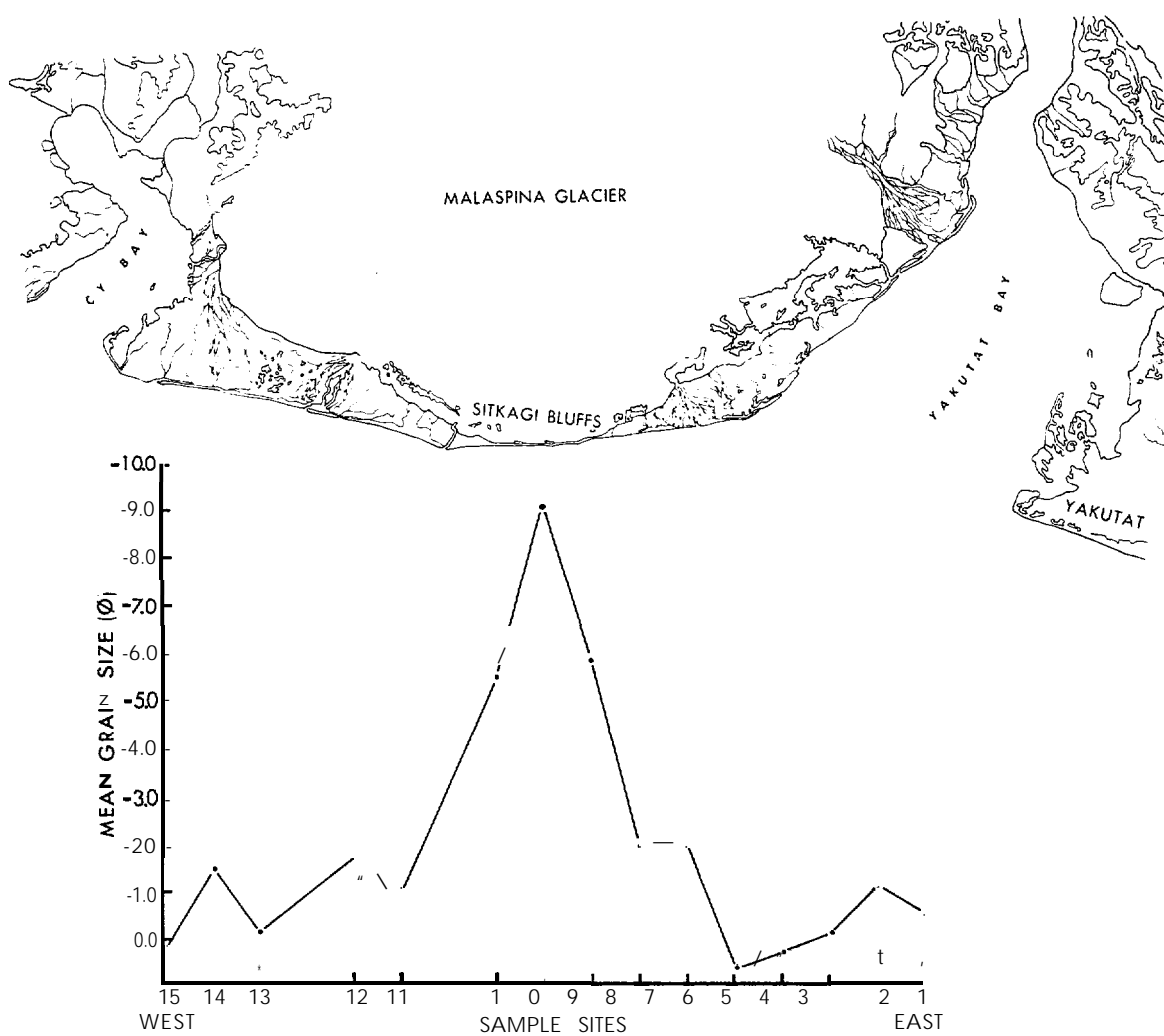


Figure 16. Graph of sediment grain size vs. position on the Malaspina Foreland. Note the fining trends to the east and west of Sitkagi Bluffs, a nodal point for sediment transport.

Nummedal and Stephen (1976) indicated that the bluffs are located at a point for transport direction. Sediments are transported both east and west from that area. Figure 16 supports that concept completely. Each of the other peaks on the graph coincides with an outwash stream outlet. These outwash systems are carrying abundant gravels, as indicated by the graph.

Discussion. - The three separate areas described above demonstrate that sediment grain size analysis can be useful in determining sediment transport trends in radically different geomorphic areas. These studies can be used to verify geomorphic indicators of transport trends as well as calculated trends using marine process parameters.

The shoreline from Cape Yakataga to Dry Bay (DBC-series area, Fig. 1) has been sub-divided into three separate areas for further discussion.

- 1) Cape Yakataga to Icy Cape (DBC-92 through DBC-80).
- 2) Pt. Riou to Grand Wash (DBC-68 through DBC-33).
- 3) Yakutat Bay to Dry Bay (DBC-32 through DBC-1).

For each of these areas, the A, B, C and D sample major and minor grain size modes were calculated and graphed. The results are shown in Figure 17. The areas are easily separated from one another using this method.

In Figure 17A, the graph for the Yakutat Foreland area, the sediments are clustered very tightly around the 1.0 ϕ to 2.0 ϕ size. There are few minor modes and more than $\frac{1}{2}$ of them are fine. This agrees with the positive skewness displayed in Figure 7. This is very close to a mono-modal distribution. This is to be expected, given the relatively constant sediment source for the area.

In Figure 17B, the graph for the Malaspina Foreland area, the sediments are far more varied with major modes occurring over the range from -3.5 ϕ to +3.0 ϕ . Minor modes display even more range of grain size. This distribution is polymodal with medium sand and fine gravel making up most of the distribution. This is to be expected across the Malaspina Foreland because of the active outwash streams carrying an abundance of mixed sand and gravel modes.

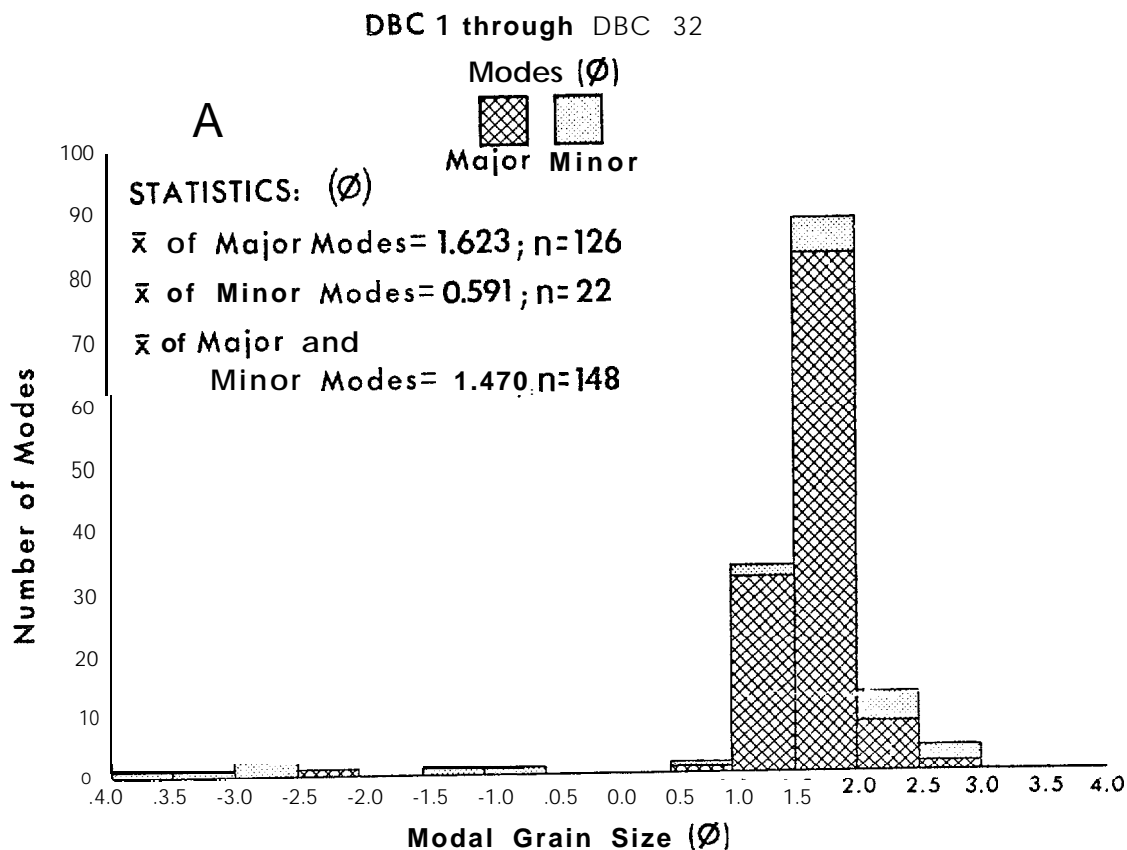
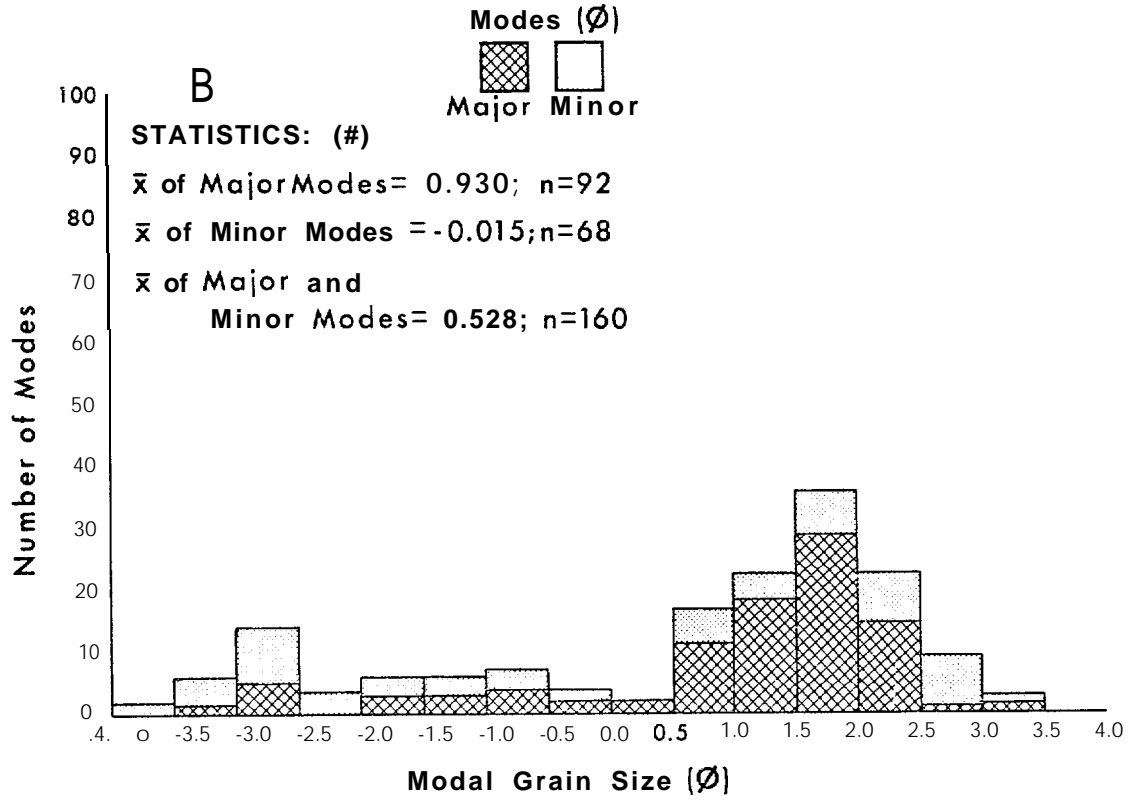


Figure 17. A. Modal grain size analysis of samples from the Yakutat Foreland. Note the bimodal nature of these sediments.

B. Modal grain size analysis of samples from the Malaspina Foreland. These samples are bimodal with a fine and coarse mode.

C. Modal grain size analysis of samples from the Yakataga - Icy Cape area. These show a highly polymodal distribution.

DBC33 through DBC 68



DBC80 through DBC92

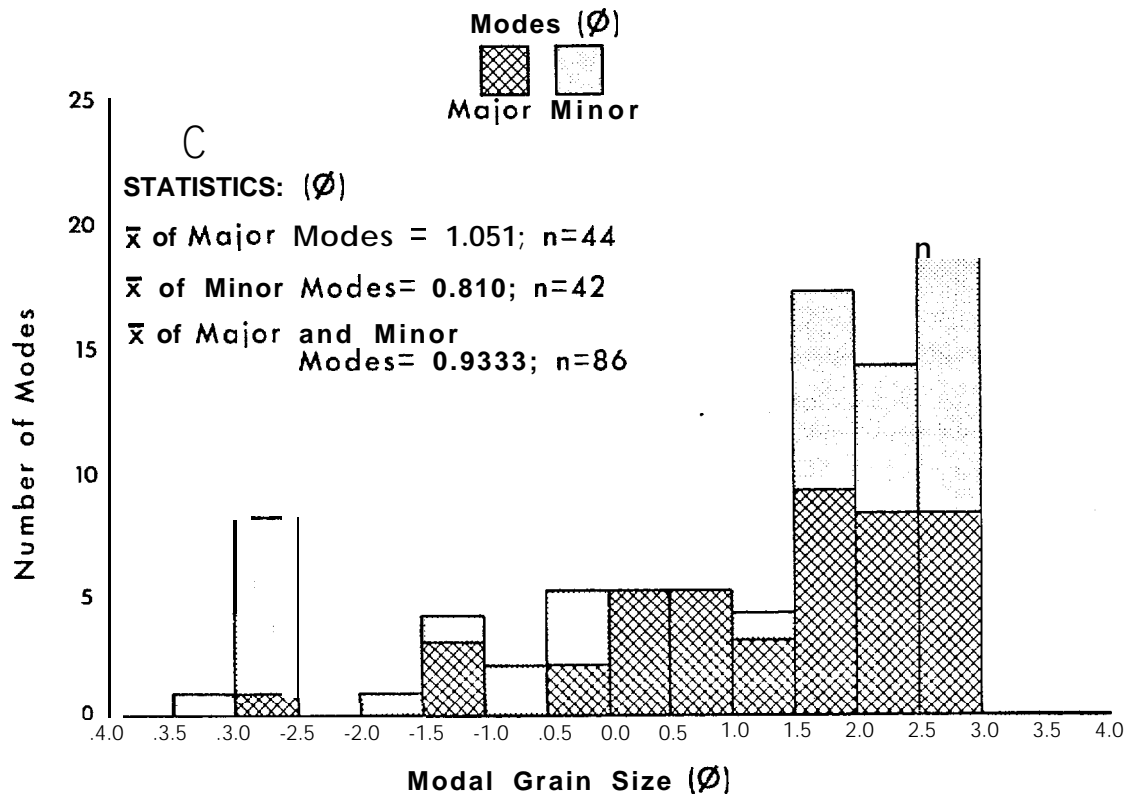


Figure 17C, the graph for the area between Icy Cape and Cape Yakataga, displays another polymodal distribution. There are almost as many minor modes as there are major modes. There are a number of active outwash streams within the area supplying coarse sediment to the system, resulting in the coarse mode. There are also areas where the beach is eroding into older beach ridge plains, thus reworking sediments, resulting in a fine sand mode. Figure 18 shows the relationship between the mean grain size of the DBC-79 through DBC-92 samples and the sorting of those samples as well as their skewness.

Thus, Figure 17 demonstrates that these areas can be distinguished from one another on the basis of grain size. The variability of the grain size is primarily a function of recent glacial history, present glacial position and drainage characteristics.

COMPOSITION

During the 1969-1970 field studies, a sample network was set up from Hinchinbrook Island to Dry Bay. At these sites, samples were taken from the middle of the beach face. These samples were later analyzed for composition. Composition was determined by analyzing 100 grains randomly selected and placing them in one of five categories:

- 1) Feldspar
- 2) Quartz
- 3) Rock fragments
- 4) Mica
- 5) Opaque heavy minerals.

The results of this analysis are given in Table 3 in the Appendix.

The sample sites have been divided into 5 separate provinces based on relatively similar geomorphic and physical process settings. They are as follows:

- 1) Copper River Delta Province: all barrier islands forming the delta as well as the spit on the east side of Hinchinbrook Island.
- 2) Controller Bay Province: Kantak Island and Okalee Spit.

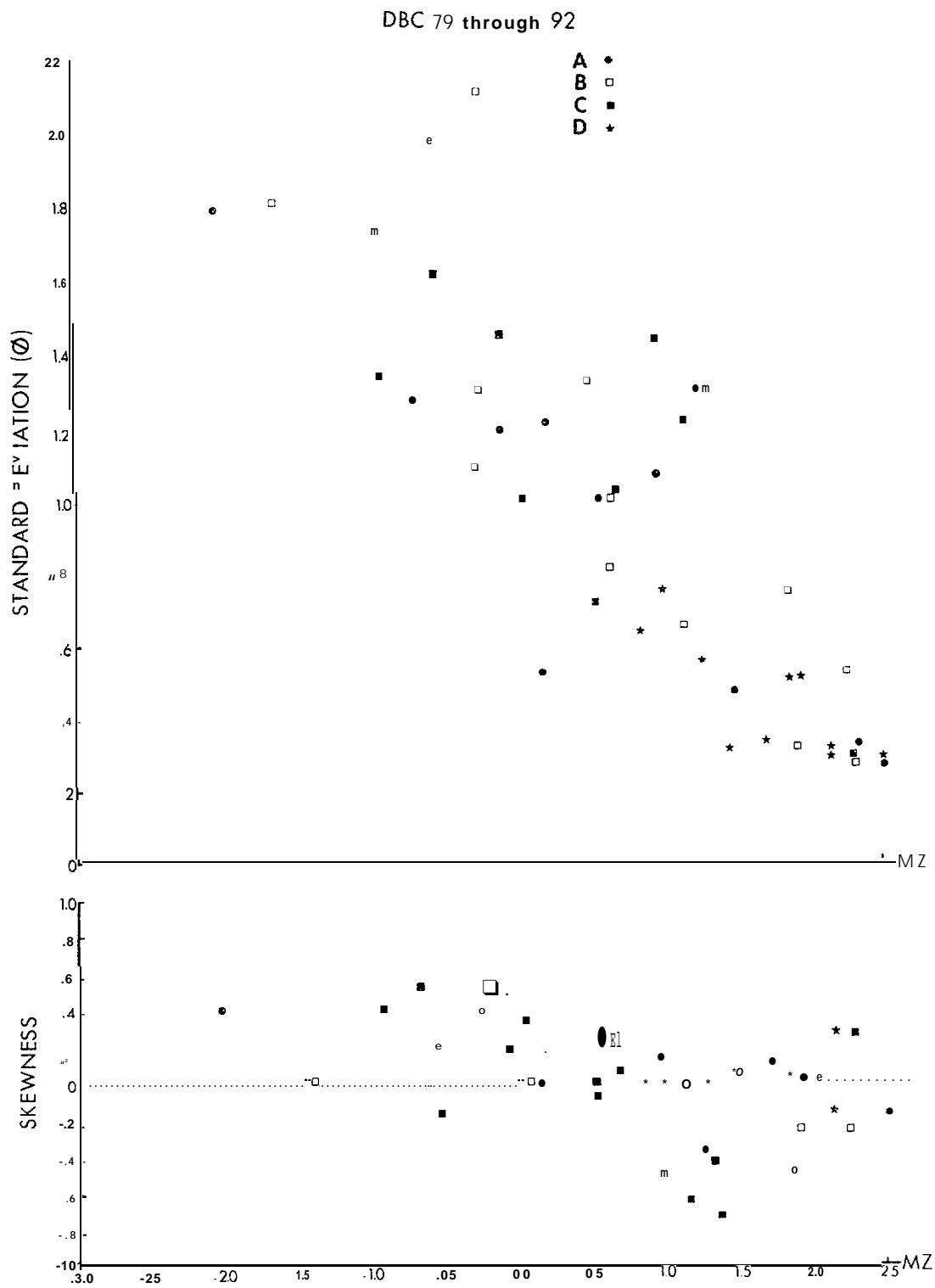


Figure 18. Graph of grain size vs. skewness and sorting for samples from the Yakataga - Icy Cape area. These samples show a high degree of variability in size and skewness.

3) Bering Foreland-Robinson Mountain Province: From Cape Suckling to Icy Bay.

4) Malaspina Foreland Province: All beaches bordering the Malaspina Glacier.

5) Yakutat Foreland Province: From Yakutat Bay to Dry Bay.

The results of the compositional analysis are given in Figure 19. This diagram is a modification from Folk (1974), using Pettijohn's (1975) maturity and provenance indexes. In this diagram, the relative percentages of quartz, feldspar, and rock fragments are used. The relative percentage of quartz to the combined feldspar and rock fragment percentage is called the maturity index*. The relative percentage of feldspar to rock fragments is called the provenance index (the lack of feldspar in these samples rendered this index non-discriminatory). It is obvious from the diagram that the provinces have distinct compositional suites.

The Copper River delta province sediments, as indicated in an earlier section, have a higher percentage of quartz than the sediments from other provinces, thus giving them a higher maturity index. They are all very similar compositionally. The Controller Bay province sediments are slightly less mature, The sediments of the Yakutat Foreland province contain still less quartz and are thus less mature than either the Copper River or Controller Bay sediments. They also show considerable variability. Using the maturity index, plotted against distance downdrift of Dry Bay, they were tested to see if they would follow the same maturing patterns demonstrated by the grain size data. Figure 20 shows the results. Note the increase in the maturity index with greater distance from Dry Bay. This agrees perfectly with the grain size trends given previously in this section. Finally, referring back to Figure 19, the Bering Glacier-Robinson Mountain sediments and the Malaspina Foreland sediments appear to have a strong compositional similarity.

* Table 4 in the Appendix presents the maturity indices for these samples.

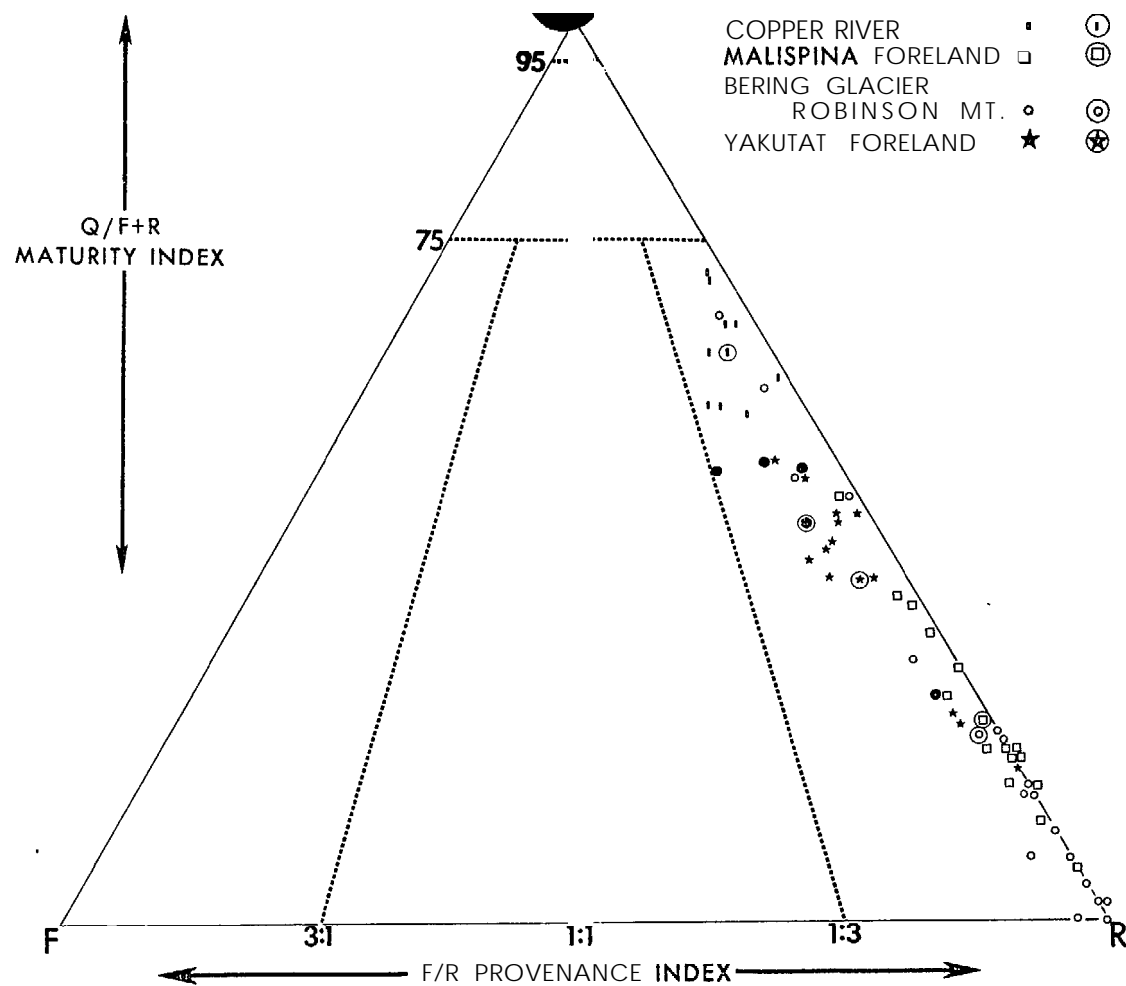


Figure 19. Compositional diagram of sediment samples from 5 areas in the Northern Gulf study area. Most samples cluster at certain points on the graph.

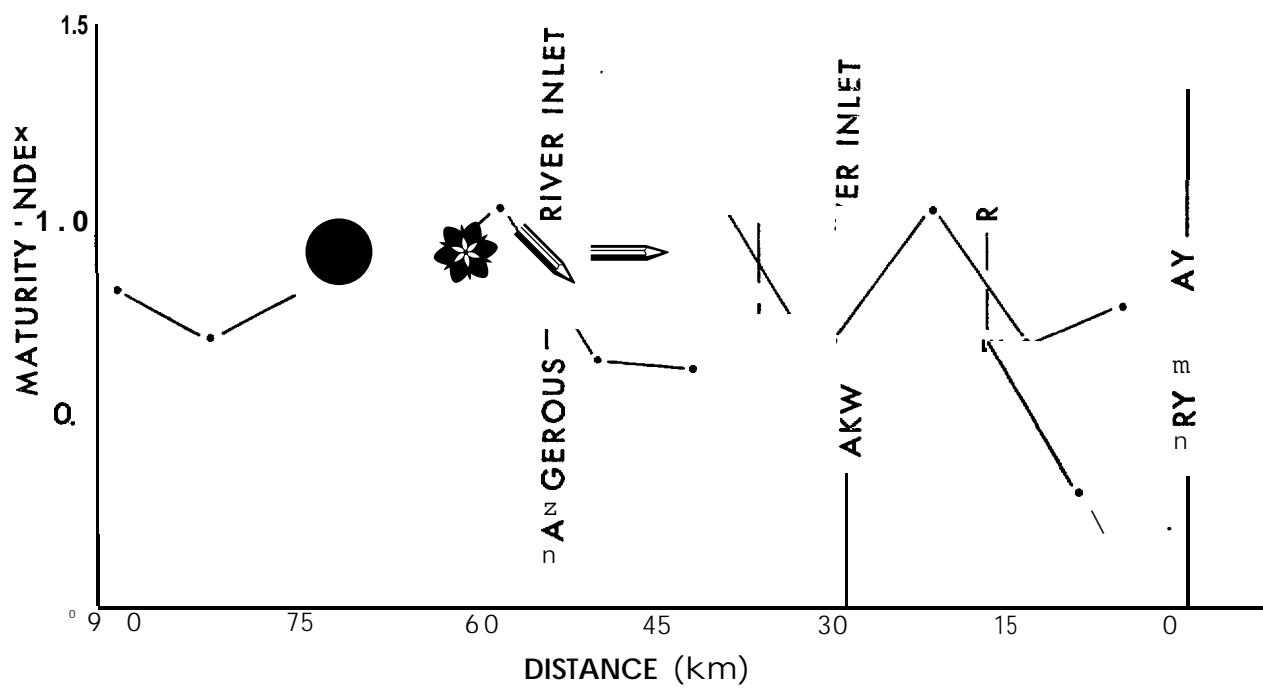


Figure 20. Graph of maturity index vs. distance downdrift of Dry Bay. Note the increase in the index with increased transport distance from the bay.

They show considerable scatter.

Figure 21 shows just the sediments from the Malaspina Foreland Province. They have been divided on the basis of distance downdrift of probable sediment sources. Note the very good correlation of increased sediment maturity with increased transport distance from sediment source. This corresponds well with concepts regarding sediment maturing compositionally with increased distance from source areas and explains the high variability of these samples.

Figure 22 shows the maturity index for the Bering Glacier - Robinson Mountain Province samples. Some interesting trends are evident. Refer to Figure 2 for locations. Moving from east to west on the diagram, a very low maturity index is located at site 29. This site is just downdrift of a glacial till exposed at Icy Cape and the Big River, both sediment suppliers. This is followed by a maturity index increase with increased distance from these sources. The White River, which is located updrift of site 26, introduces immature sediment into the system; these sediments mature with increasing distance downdrift of the river, finally terminating with a high maturity index at the end of the Duktoth River Spit. From there to Cape Suckling, the outwash streams draining the Bering Glacier introduce an immature sediment suite to the coast.

This section has analyzed the sediment samples collected during two separate field studies. This analysis follows closely accepted patterns for sediment dispersal and maturing. The study area is extremely diverse with regard to coastal geomorphology and the balance between marine and terrestrial processes. However, even with this complexity, trends in sediment transport are present which verify geomorphic and process indicators of dominant sediment transport direction as well as visual estimates of sediment sources.

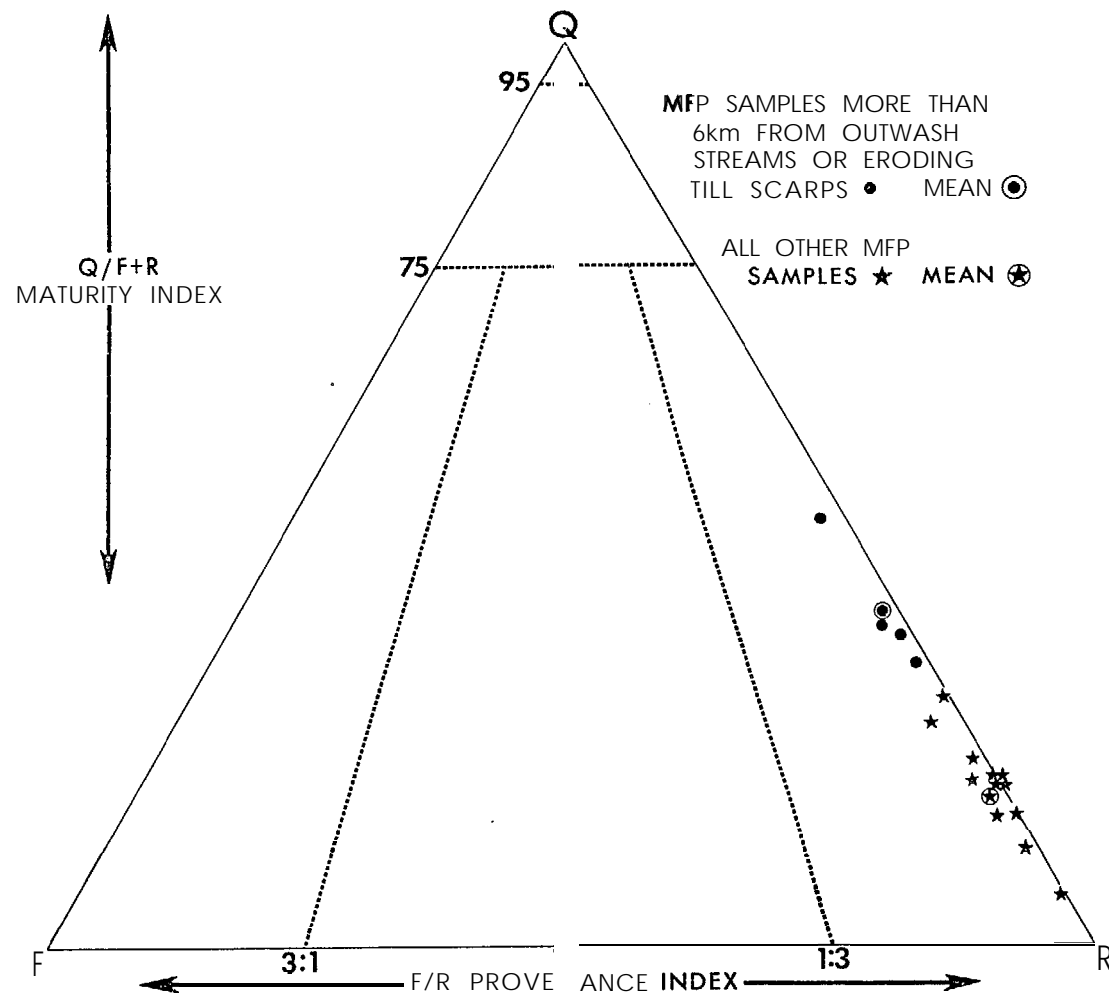


Figure 21. Compositional graph of Malaspina Foreland Province samples separated on the basis of distance from sediment sources. The samples 6km or more from their sediment sources have a higher percentage of quartz.

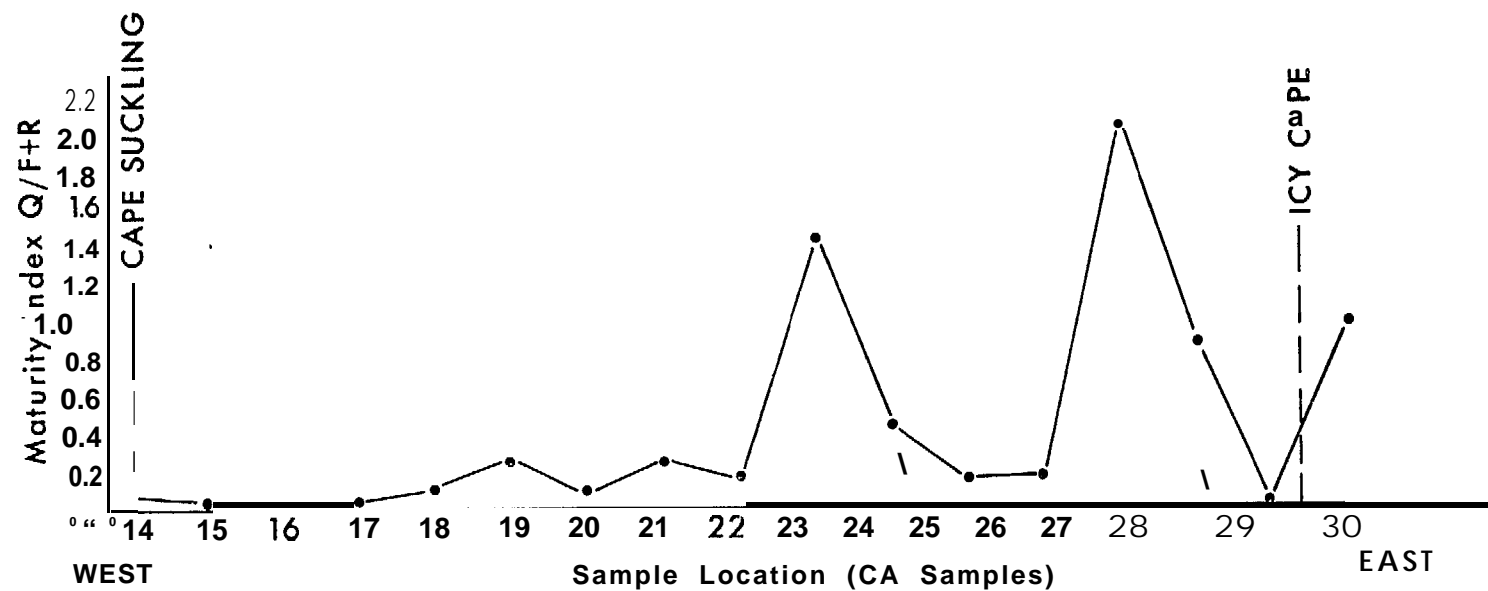


Figure 22. Graph of maturity index vs. position on the Bering Glacier - Robinson Mountain Province. The more mature sediments are at the ends of spits far from sediment sources. See discussion in text.

REFERENCES CITED

- Folk, R. L., 1968, Petrology of sedimentary rocks: Hemphill's, Austin, Texas, 170 p.
- Folk, R. L., 1974, Petrology of sedimentary rocks, Hemphill Publishing Company, Austin, Texas 182 p.
- Folk, R. L., and Ward, W. C., 1957, Brazes River point bar: a study in the significance of grain size parameters: Jour. Sed. Pet., v. 27, No. 1, p. 3-26.
- Hayes, M. O., et al., 1969-1970, Field work done in the Northern Gulf of Alaska.
- Nun-medal, D., et al., 1974, Recent migrations of the Skeidararsandur shoreline, southeast Iceland, Final Rept. to Naval Ordnance Laboratory, Univ. of Mass, 182 p.
- Nummedal, D., and Stephen, M. F., 1976, Coastal dynamics and sediment transportation, Northeast Gulf of Alaska, Tech. Rept. No. 9-CRD, Dept. of Geol., U.S.C., 148 p.
- NODC (National Ocean Data Center) 707 A Street, Anchorage, Alaska, 99501
- Pettijohn, F. J., 1975, Sedimentary rocks, 3rd ed., Harper and Row, Publishers, N. Y., N. Y., 628 p.
- Winkelmolen, A. M. and Veenstra, H. J., 1974, Size and shape sorting in a Dutch tidal inlet, Sedimentology, v. 21, No. 1, p. 107-126.

Project 2. Shoreline of Kotzebue Sound (Cape Prince of Wales to Point Hope)

a) Field and Laboratory Activities

No field work has been carried out on this project since the 1976 summer field season. Laboratory analysis of sediment samples is underway as well as computer storage of each profile measured during July - August, 1976. Additionally, Christopher H. Ruby and Larry G. Ward, both members of the 1976 field team, traveled to the Buzzards Bay, Massachusetts oil spill. Detailed descriptive data regarding oil spills in ice bound environments was collected. Shortly after that spill, the Ethyl H., a barge carrying #6 fuel oil, was holed in the Hudson River. Since there was considerable ice on the river at that time, C. H. Ruby and Erich Gundlach spent a few days in the field analyzing the interaction of the oil and ice as well as the constraints placed on the clean up operation by the oil. These two field studies supported by USC funds, have provided considerable insight into oil spills in arctic and near arctic areas. This information will be used to formulate an oil spill vulnerability scheme for Kotzebue Sound, after the ice studies we have planned for the Sound this year are completed.

APPENDIX

Table 1 -- Grain Size Parameters

Table 2 -- Modal Grain Size Parameters

Table 3 -- Compositional Data

Table 4 -- Maturity Indices

TABLE 1

<u>Photo</u>	<u>Mean (ϕ)</u>	<u>Standard Deviation (#)</u>	<u>Skewness (ϕ)</u>
BC-1			
A-U.B.F.	1.590	0.287	0.056
B-L.H.T.S.	1.370	0.233	0.059
C-Neap Berm	0.394	1.162	0.567
D-W.S. Dune	1.640	0.264	0.116
BC-2			
A-Spring H.T.B.F.	1.535	0.271	0.147
B-L.H.T.S.	0.177	1.747	-0.687
C-M.B.F.	0.380	1.398	-0.436
D-W.S. Dune	1.645	0.313	-0.061
BC-3			
A-Berm Runnel *	1.627	0.546	0.277
B-Neap Berm	0.401	1.542	-0.577
C-L.B.F.	-0.700	1.137	-0.026
D-W.S. Dune	1.244	0.232	0.154
BC-4			
A-Berm Top	1.397	0.294	0.071
B-Berm Crest	1.446	0.278	-0.002
C-L.B.F.	1.312	0.509	-0.157
D-W.S. Dune	1.459	0.306	0.038
BC-5			
A-Berm Top	1.862	0.197	-0.003
B-Berm Crest	1.335	0.275	0.095
C-L.B.F.	1.236	0.308	0.187
D-W.S. Dune	1.412	0.243	-0.086
BC-6			
A-Berm Top	1.306	0.315	-0.049
B-Berm Crest	1.192	0.363	0.070
C-L.B.F.	1.155	0.382	-0.046
D-W.S. Dune	1.193	0.235	-0.059
3C-7			
A-Runnel	1.719	0.263	0.086
B-Berm Top	1.194	0.289	0.094
C-L.B.F.	1.303	0.295	0.157
D-W.S. Dune	1.620	0.334	-0.087
3C-8			
A-U.B.F.	1.735	0.257	0.127
B-Berm Runnel	1.418	0.323	0.206
C-Neap Berm Top	1.339	0.301	0.181
D-W. S. Dune	1.734	0.282	0.073
3C-9			
A-U.B.F.	1.489	0.263	0.122
B-Runnel	1.169	0.263	0.135
C-L.B.F.	1.324	0.310	0.236
D-W.S. Dune	1.803	0.270	0.058

	<u>Mean (ϕ)</u>	<u>Standard Deviation (ϕ)</u>	<u>Skewness (ϕ)</u>
BC-10			
A-U.B.F.	1.458	0.269	0.088
B-Neap Berm	1.276	0.336	0.172
C-Runnel	1.241	0.356	0.176
D-Low Dune Ridge	1.907	0.323	0.018
BC-11			
A-U.B.F.	1.880	0.258	0.127
B-Runnel	1.284	0.277	0.139
C-L.B.F.	1.581	0.313	0.048
D-High Dune Ridge	1.802	0.298	0.037
BC-12; Hq-2			
A-M.B.F.	1.446	0.287	0.006
B-Runnel Edge	1.437	0.333	0.214
C-Ridge Crest	1.432	0.329	0.116
D-Flat Dune	1.878	0.265	0.025
BC-13			
A-U.B.F.	2.083	0.239	0.158
B-M.B.F.	1.832	0.253	0.223
C-L.T.T.	1.679	0.299	0.120
D-High Dune Ridge	1.970	0.263	0.052
BC-14			
A-U.B.F.	2.065	0.245	0.308
B-M.B.F.	1.928	0.246	0.099
C-L.T.T.	1.742	0.219	0.229
D-W.S. Dune	2.128	0.256	0.114
BC-15			
A-Runnel	2.072	0.247	0.246
B-M.B.F.	1.619	0.263	0.174
C-L.B.F.	1.630	0.292	0.166
D-W.S. Dune	2.071	0.269	0.093
BC-16			
A-U.B.F.	1.701	0.270	0.126
B-Ridge Crest	1.741	0.312	0.082
C-L.B.F.	1.724	0.301	-0.058
D-W.S. Dune	1.893	0.329	0.232
BC-17			
A-U. Ridge Top	1.779	0.281	0.161
B-L. Ridge Top	1.389	0.340	0.055
C-L.B.F.	1.833	0.336	0.078
D-W.S. Dune	1.909	0.320	0.191
BC-18			
A-U.B.F.	2.135	0.280	0.200
B-Ridge Top	1.695	0.352	0.066
C-Ridge Top	1.651	0.353	0.096
D-W.S. Dune	2.037	0.296	0.101

	<u>Mean (ϕ)</u>	<u>Standard Deviation (ϕ)</u>	<u>Skewness (ϕ)</u>
BC-19			
A-U.B.F.	1.872	0.258	0.141
B-Ridge Top	1.861	0.338	0.230,
C-L.B.F.	1.267	0.503	-0.270
D-W. S. Dune	1.905	0.299	0.169
BC-20			
A-U.B.F.	1.871	0.260	0.118
B-L.T.T.	1.751	0.220	0.168
C-L.T.T.	1.560	0.268	0.063
D-Dune Ridge	2.079	0.251	0.073
BC-21			
A-U.B.F.	1.891	0.232	-0.064
B-L.B.F.	1.813	0.239	0.216
C-Ridge	1.860	0.327	0.209
D-Dune	1.940	0.301	0.115
EC-22			
A-U.B.F.	1.929	0.285	0.117
B-L.B.F.	1.765	0.271	0.188
C-L.T.T.	1.152	0.385	0.210
D-High Dune Ridge	2.065	0.280	0.083
BC-23			
A-U.B.F.	2.151	0.299	0.206
B-Runnel	1.890	0.303	0.178
C-Ridge Top	1.926	0.291	0.097
BC-24			
A-U.B.F.	1.663	0.351	0.140
B-L.B.F.	-0.010	1.575	-0.371
C-L.T.T.	1.629	0.287	0.146
D-W.S. Dune	1.918	0.262	0.014
BC-25			
A-U.B.F.	1.902	0.253	0.088
B-Ridge Top	1.755	0.281	0.114
D-Flat Dune	2.024	0.233	0.145
BC-26			
A-U.B.F.	1.894	0.266	0.160
B-L.B.F.	1.743	0.262	0.153
C-Ridge Top	1.661	0.293	0.101
D-W.S. Dune	2.094	0.227	0.065
BC-27			
A-U.B.F.	2.030	0.218	0.247
B-L.B.F.	1.832	0.298	0.138
C-Ridge Top	1.881	0.305	0.225
D-W.S. Dune	1.826	0.303	0.138

<u>Photo</u>	<u>Mean (ϕ)</u>	<u>Standard Deviation (ϕ)</u>	<u>Skewness (ϕ)</u>
BC-28			
A-U.B.F.	2.136	0.270	0.182
B-L.T.T.	1.868	0.265	0.144
C-Ridge Top	2.054	0.319	0.122
D-W.S. Dune	1.936	0.249	0.079
BC-29			
A-U.B.F.	1.994	0.235	0.179
B-L.T.T.	1.799	0.296	0.231
C-L.T.T.	1.843	0.303	0.181
D-W.S. Dune	1.893	0.253	0.086
BC-30			
A-U.B.F.	2.002	0.220	0.145
B-M.B.F.	1.998	0.235	0.157
c-Low Ridge	1.749	0.257	0.119
D-W.S. Dune	2.190	0.249	0.113
BC-31			
A-U.B.F.	2.245	0.405	0.073
B-M.B.F.	2.023	0.421	0.103
C-L.B.F.	2.025	0.681	-0.176
BC-32			
A-Runnel	2.132	0.288	0.191
B-M.B.F.	2.125	0.317	0.278
C-Ridge	1.045	0.342	0.195
BC-33			
A-M.B.F.	2.179	0.525	-0.004
B-L.T.T.	2.587	0.415	0.151
C-L.T.T.	2.545	0.266	0.383
D-W.S. Dune	-0.291	2.117	-0.079
BC-34			
A-M.B.F.	2.116	0.801	-0.592
B-L.T.T.	2.819	0.393	0.132
C-L.T.T.	2.332	0.995	-0.533
D-Low Dune	1.346	0.718	-0.319
BC-35			
A-M.B.F.	1.405	0.788	-0.248
B-L.T.T.	2.241	0.670	-0.369
C-L.T.T.	2.313	0.599	-0.054
D-W.S. Dune	2.377	0.526	0.166
C-36			
A-U.B.F.	1.983	0.367	0.116
C-L.T.T.	0.166	1.726	0.063
D-W.S. Dune	1.021	0.698	0.043

*

	<u>Photo</u>	<u>Mean (ϕ)</u>	<u>Standard Deviation (ϕ)</u>	<u>Skewness (ϕ)</u>
BC-37				
	A-Berm Crest	1.517	0.374	-0.057
	B-M.B.F.	1.364	0.542	0.177
	C-L.B.F.	1.667	0.693	0.004
BC-38				
	A-Berm Top	1.337	0.523	0.175
	B-M.B.F.	0.114	2.006	-0.044
	C-Ridge Top	1.739	0.468	0.008
BC-39				
	A-U.B.F.	1.813	0.517	0.016
	B-M.B.F.	1.985	0.492	0.047
BC-40				
	A-M.B.F.	1.484	0.575	-0.078
	B-L.B.F.	2.002	0.395	0.119
	C-L.B.F.	2.189	0.411	0.166
	D-W.S. Dune	0.613	0.794	0.110
BC-41				
	A-U.B.F.	1.689	0.434	0.077
	B-M.B.F.	1.885	0.855	-0.322
	C-L.B.F.	2.084	0.511	-0.037
	D-W.S. Dune	1.636	0.522	-0.077
BC-42				
	A - Berm	1.966	0.367	0.060
	B-M.B.F.	1.733	0.486	0.086
	C-L.B.F.	-0.113	0.987	0.002
	D-W.S. Dune	0.663	0.636	-0.036
BC-43				
	A-Berm Crest	2.268	0.783	-0.251
	B-U.B.F.	0.226	1.886	-0.490
	C-L.B.F.	1.686	0.524	0.125
	D-W.S. Dune	1.169	0.793	-0.206
BC-44				
	A-Berm Top	0.421	1.687	-0.301
	B-L.B.F.	1.986	0.553	0.017
	C-L.B.F.	0.893	1.237	-0.175
	D-Dune Ridge	1.494	0.371	0.040
BC-45				
	A-U.B.F.	1.649	0.370	0.027
	B-Neap Berm	1.572	0.515	0.103
	C-L.B.F.	0.634	0.843	0.071
	D-W.S. Dune	1.508	0.265	0.100

	<u>Photo</u>	<u>Mean (ϕ)</u>	<u>Standard Deviation (ϕ)</u>	<u>Skewness (ϕ)</u>
BC-46				
A-U.B.F.	*	-1.948	1.309	0.068
B-Runnel		1.625	0.077	-0.000
C-Ridge		2.228	0.461	0.252
D-Dune Ridge		1.619	0.377	0.098
BC-47				
A-Berm Crest		1.165	0.392	0.013
C-L.B.F.	*	-1.032	1.541	0.226
BC-48; Mal-3		0.629	0.657	0.015
A-Storm Beach	*	0.629	0.657	0.015
B-Berm Top		-2.183	1.044	0.122
C-L.B.F.	*			
D-W.S. Dune		-1.329	0.591	0.422
BC-49				
A-Berm Top		1.322	0.498	0.283
B-U.B.F.		0.854	0.324	-0.002
C-L.B.F.	*			
BC-50				
A-U.B.F.	*	1.208	0.461	0.318
B-M.B.F.	*			
C-L.B.F.		-1.343	1.717	0.146
D-W.S. Dune		1.194	0.452	0.309
BC-51				
A-U.B.F.	*			
B-M.B.F.	*			
C-L.B.F.	*			
BC-52				
A-U.B.F.	*			
B-M.B.F.	*			
C-L.B.F.	*	0.769	1.054	-0.006
BC-57				
A-U.B.F.		1.240	0.518	0.235
B-M.B.F.	*			
C-L.B.F.	*	0.339	1.708	-0.292
D-W.S. Dune		1.268	0.301	0.207
BC-58				
A-U.B.F.	*	1.495	0.363	0.154
B-M.B.F.	*			
C-Berm Face	*	-2.597	1.585	0.546
D-Dune Ridge		1.031	0.363	0.128

	<u>Photo</u>	<u>Mean (ϕ)</u>	<u>Standard Deviation (ϕ)</u>	<u>Skewness (ϕ)</u>
BC-59				
A-Storm Berm Face	*			
B-M.B.F.	*	-0.424	1.176	0.263
C-L.B.F.	*	-0.753	1.562	0.038
BC-60; Mal-2				
A-Spring Berm	*			
B-M.B.F.	*	1.650	0.441	-0.105
C-Neap Berm	*			
D-Grassy Dunes		1.142	0.441	-0.058
BC-61				
A-U.B.F.	*			
B-Berm	*	0.351	1.380	0.471
C-L.B.F.	*	0.128	1.449	0.350
D-W.S. Dune		1.419	0.679	0.065
BC-62				
A-U.B.F.	*			
B-Berm	*			
C-L.B.F.	*	0.525	1.488	-0.045
D-W.S. Dune		1.898	0.354	0.060
BC-63				
A-High Berm	*	0.348	1.522	-0.227
B-Mid Berm	*			
C-L.B.F.	*	0.028	1.517	0.286
BC-64				
A-High Berm	*	1.305	1.080	-0.383
B-Low Berm	*			
C-L.B.F.	*			
BC-65				
A-Berm Top		1.721	0.650	-0.054
B-Low Berm	*			
C-L.B.F.	*	-1.022	2.163	0.374
BC-66				
A-U.B.F.	*			
B-M.B.F.	*			
C-L.B.F.	*	0.483	1.607	-0.248
BC-67				
A-Berm Runnel		0.662	1.158	0.103
B-Low Berm Crest		1.187	1.068	-0.304
C-Berm Cusp				
BC-68				
A-Berm Top		-1.557	1.137	0.237
B-Lower Berm				
C-L.B.F.		-2.232	1.365	0.681

	<u>Photo</u>	<u>Mean (ϕ)</u>	<u>Standard Deviation (ϕ)</u>	<u>Skewness (#)</u>
BC-69				
A-U.B.F.	*			
B-Berm Runnel	*			
C-L.B.F.	*			
BC-71				
A-U.B.F.	*	1.694	0.487	0.047
B-M.B.F.	*	0.069	1.757	-0.434
C-L.B.F.	*	1.533	0.634	-0.115
D-Wind Lag		1.215	0.658	-0.112
BC-72				
A-Berm Top		1.439	0.518	-0.058
B-Berm Crest	*	1.588	0.533	-0.028
C-L.B.F.	*	0.691	1.234	-0.336
D-W.S. Dune		1.723	0.540	-0.041
BC-73				
A-L.H.T.S.		2.200	0.535	-0.240
B-M.B.F.		2.439	0.350	-0.323
C-Low Berm Cusp	*	2.271	0.469	-0.225
BC-75				
A-L.H.T.S.		0.355	1.641	-0.343
B-L.T.T.		0.987	1.380	-0.564
C-L.T.T.		2.097	0.555	-0.126
D-W.S. Dune		1.819	0.610	-0.106
C-76				
A-Berm Top		1.169	0.517	-0.047
B-Spring Berm Crest	*	1.484	1.113	-0.378
C-Spring Berm Base	*	0.534	0.982	-0.155
D-W.S. Dune		2.651	0.479	-0.052
C-77				
A-U.B.F.	*			
B-M.B.F.	*			
C-L.B.F.	*	-0.437	1.156	-0.149
C-78				
A-U.B.F.	*			
B-Gravel Horn	*			
C-L.B.F.	*	-0.782	1.750	-0.191
C-79				
A-U.B.F.	*	-2.022	1.798	0.401
B-L.T.T.	*	-1.626	1.811	-0.081
C-L.T.T.	*	-0.914	1.738	-0.148
D-W.S. Dune		1.297	0.558	-0.017

	<u>Photo</u>	<u>Mean (ϕ)</u>	<u>Standard Deviation (ϕ)</u>	<u>Skewness (ϕ)</u>
BC-80				
	A-L.H.T.S.	0.238	1.211	0.186
	C-L.T.T.	-0.062	1.441	0.175
	D-Dune Ridge	1.719	0.309	0.095
BC-81				
	A-L.H.T.S.	*		
	B-M.B.F.	*		
	C-L.B.F.	*		
	D-W.S. Dune	-0.528	1.614	-0.186
		1.488	0.304	0.034
BC-82				
	A-Berm Top	0.574	0.999	0.185
	B-M.B.F.	1.933	0.306	-0.259
	C-Ridge Top	0.514	1.325	0.016
	D-W.S. Dune	1.016	0.754	-0.002
BC-83				
	A-L.H.T.S.	2.340	0.320	0.066
	B-Runnel Edge	1.870	0.740	-0.314
	C-Ridge Top	0.996	1.438	-0.500
	D-Low Dune	2.518	0.284	-0.202
BC-84				
	B-L.B.F.	2.318	0.264	0.361
	C-L.T.T.	2.300	0.287	0.264
	D-W.S. Dune	2.156	0.294	-0.167
BC-85; YKG-3				
	A-H.T.S.			
	B-Welded Ridge			
	C-Ridge Top	1.169	1.212	-0.668
	D-W.S. Dune	2.165	0.307	0.266
BC-86				
	A-U.B.F.	2.506	0.263	-0.191
	B-Ridge Top	-0.233	2.102	0.022
	C-Ridge Top	1.387	1.628	-0.747
BC-87				
	A-M.B.F.	0.171	0.538	0.072
	B-Ridge Crest	2.257	0.524	-0.286
	C-Ridge Top	1.328	1.299	-0.449
BC-88				
	A-Gravel Cusp	-0.098	1.194	0.467
	B-M.B.F. Horn	0.537	1.015	0.230
	C-L.B.F.	-0.059	0.983	0.328
BC-89				
	A-Berm Top	-0.536	1.968	0.201
	B-Berm Face	-0.276	1.081	0.409
	C-Low Berm Face	-0.684	1.272	0.524

	<u>Photo</u>	<u>Mean (ϕ)</u>	<u>Standard Deviation (#)</u>	<u>Skewness (ϕ)</u>
BC-90				
A-U.B.F.	*	1.278	1.287	-0.386
B-Berm Top	*	-0.230	1.289	0.552
C-L.B.F.	*	-0.914	1.347	0.405
D-W.S. Dune		1.960	0.514	0.029
DBC-91				
A-U.B.F.		0.982	0.926	0.127
B-M.B.F.		0.655	0.806	0.241
C-L.B.F.		0.688	1.002	0.063
D-W.S. Dune		0.867	0.637	-0.014
DBC-92				
A-U.B.F.	*	1.503	0.469	-0.027
B-L.T.T. Runnel	*	1.165	0.645	-0.052
C-L.T.T. Ridge	*	0.546	0.708	-0.077
D		1.883	0.505	-0.004
DBC-93				
A-L.H.T.S.	*	2.409	0.386	-0.171
DBC-101				
A-High Berm Crest	*			
B-Mid Berm Crest	*			
C-Neap Berm Crest	*	-1.279	0 . 7 4 3	-0.319
BC-102				
A-L.H.T.S.	*	-0.397	2.244	-0.779
B-Berm Face	*			
C-Berm Crest	*	-2.094	1.185	-0.193
DBC-103				
A-H.H.T.S.	*	2.352	0.485	-0.074
B-M.B.F.	*	2.297	0.516	0.149
C-L.B.F.	*	-0.074	2.520	-0.621
DBC- 104				
A-H. Berm Top	*			
B-M.B.F.	*			
C-L.B.F.	*	-0.528	2.675	0.098
DBC-105				
A-H. Berm Crest	*			
B-M.B.F.	*			
C-L.B.F.	*			
c-106				
A-M.B.F.		-2.328	1.373	0.365
B-L.T.T.				
C-L.T.T.				

PERMANENT PROFILES

	<u>Mean</u>	<u>St. Dev.</u>	<u>Skew</u>
Eg1 A	2.320	0.254	0.100
B	2.356	0.280	0.187
D	2.306	0.367	0.079
Eg3 C	2.270	0.296	0.282
D	2.293	0.249	0.354
Eg4 A	2.094	0.288	0.070
B	2.305	0.240	0.292
Eg8 A	2.106	0.564	0.115
B	2.324	0.448	0.213
c	1.675	0.748	0.049
Sr1 A	2.323	0.316	0.315
B	1.525	0.991	-0.226
c	1.813	0.452	0.032
D	2.031	0.420	0.096
Knk1 A	2.809	0.382	0.016
B	1.351	0.383	-0.104
c	2.992	0.307	-0.170
D	2.911	0.302	0.030
Ok1 A	2.110	0.374	0.163
Seal A	1.498	0.410	0.042
B	1.813	0.394	-0.027
c	0.996	0.445	0.182
Ykg2 C	1.344	0.979	-0.379
D	2.047	0.358	0.219
Ykg3 c	1.169	1.212	-0.668
D	2.165	0.307	0.266
Ma12 B	1.650	0.441	-0.105
D	1.142	0.441	-0.058
Ma13 A	0.629	0.657	0.015
B	-2.183	1.044	0.122
c	-0.823	1.268	-0.283
D	-1.329	0.591	0.422
Hq2 A	1.446	0.287	0.006
B	1.437	0.333	0.214
c	1.472	0.329	0.116
D	1.878	0.265	0.025

TABLE 2

MODES (ϕ)

	<u>Major</u>	<u>Major</u>	<u>Minor</u>	<u>Minor</u>
DBC-1A	1.625			
B	1.375			
c	1.625			
DBC-2A	1.375			
B	1.125		-3.375	
c	1.375		-2.625	0.875
D	1.625			
DBC-3B	1.375		-2.625	1.875
c	-2.125			
D	1.125		-1.125	0.625
DBC-4A	1.375			
B	1.375			
c	1.375			
D	1.375			
DBC-5A	1.875			
B	1.125			
c	1.125		1.625	
D	1.500			
DBC-6A	1.375			
B	1.125			
c	1.125			
D	1.125			
DBC-7A	1.625			
B	1.125			
c	1.125			
D	1.875		1.375	
DBC-8A	1.625			
B	1.125			
c	1.125			
D	1.625			
DBC-9A	1.375			
B	1.125			
c	1.125			
D	1.625			
DBC10A	1.375			
B	1.125			
C	1.125			
D			1.625	2.125

	<u>Major</u>	<u>Major</u>	<u>Minor</u>	<u>Minor</u>
DBC-11A	1.875			
B	1.125			
C	1.625			
D	1.875	1.625		
DBC-12;				
HQ2A	1.625			
B	1.125		1.875	
C	1.375			
D	1.625		2.125	
DBC- 13A			2.125	1.875
B	1.625			
C	1.625			
D	1.875			
DBC-14A	1.875			
B	1.875			
C	1.625			
D	2.125			
DBC-15A	1.875			
B	1.625			
C	1.625			
D	1.875			
DBC-16A	1.625			
B	1.625			
C	1.875			
D	1.875		2.375	
DBC-17A	1.625			
B	1.375			
C	1.875	1.625		
D	1.875	1.625		
DBC- 18A	2.125			
B	1.625			
C	1.625			
D	1.875			
DBC-19A	1.875			
B	1.625			
C	1.375			
D	1.625			
DBC- 20A	1.875			
B	1.625			
C	1.625			
D	1.875			
DBC-21A	1.875			
B	1.625			
C	1.875	1.625		
D	1.875			

	<u>Major</u>	<u>Major</u>	<u>Minor</u>	<u>Minor</u>
DCB-22A	1.875			
B	1.625			
c	0.875			
D	2.125	1.875		
DBC-23A	1.875			
B	1.875			
c	1.875			
DBC-24A	1.625		2.125	
B	1.125		-3.625	-2.625
c	1.625			
D	1.875			
DBC- 25A	1.875			
B	1.625			
D	1.875			
DBC- 26A	1.875			
B	1.625			
c	1.625			
D	2.125			
DBC-27A	1.875			
B	1.625			
c	1.875			
D	1.625			
DBC-28A	2.125			
B	1.875			
c	1.875			
D	1.875			
DBC-29A	1.875			
B	1.625			
c	1.625			
D	1.875			
DBC-30A	1.875			
B	1.875			
c	1.625			
D	2.125			
DBC-31A	2.625	2.125		
B	1.875		2.625	
c	1.875		2.625	
DBC-32A	2.125			
B	1.875		2.875	
c	1.875			
DBC- 33A	2.625		1.875	
B	2.375			
c	2.375			
D	1.875		-0.875	-3.125

,'

	<u>Major</u>	<u>Major</u>	<u>Minor</u>	<u>Minor</u>
DBC-34A	2.375		1.375	
B	2.625			
c	2.375		-2.125	
D	1.625		0.375	
DBC-35A	1.700		.700	
B	2.375		1.875	-3.875
c	2.125			
D	2.125			
DBC-36A	1.875			
c	-0.375		2.375	-3.125
D	1.125		0.375	
DBC-37A	1.625			
B	1.125			
c	1.125		2.125	
DBC-38A	1.125			
B	-0.875		-2.625	2.625
c	1.375	1.875		
DBC-39A	2.125			
B	1.875			
DBC-40A	1.625		0.875	
B	1.875			
c	2.125.			
D	0.625		0.125	
DBC-41A	1.625			
B	2.125		2.625	
c	2.125			
D	1.875		2.375	
DBC-42A	1.875			
B	1.625			
c	0.125	0.625	-2.125	2.375
D	0.625			
DBC-43A	2.375		0.625	
B	1.375		-2.625	
c	1.625			
D	1.875		0.450	-3.875
DBC- 44A	1.625	0.875	-0.875	-2.625
B	2.125			
c	1.375	0.875	2.625	-2.625
D	1.375			
DBC-45A	1.625			
B	1.625	1.125		
c	0.625		2.375	
D	1.375			

	<u>Major</u>	<u>Major</u>	<u>Minor</u>	<u>Minor</u>
DBC-46A	-2.625		-1.375	-3.125
B	1.625			
C	2.125	-1.875	3.125	
D	1.625			
DBC-47A	1.125		1.625	
B	-1.375		1.375	-2.625
DBC-48;				
Mal 3 A	0.625			
B	-2.625		-2.125	0.875
C	0.125	-0.875	-2.125	-3.375
D	1.625		1.375	
DBC-49A	1.125			
B	0.875			
DBC-50A	1.950		2.125	
C	-1.625		0.875	-2.625
D	0.875			
DBC-52C	0.375		1.625	
DBC-57A	1.125			
C	0.875		-1.875	-2.875
D	1.125			
DBC-58A	1.375			
C	-2.625		-3.125	-1.625
D	-0.875			
DBC-59B	-0.625		-1.875	
C	-0.875		-2.625	
DBC-60 ;				
Mal 2 B	1.875			
D	1.125			
DBC-61B	-0.625		2.625	
C	-1.125		1.875	2.375
D	1.375		2.625	
DBC-62C	0.875		-0.875	2.625
D	1.875			
DBC-63A	1.600		-2.625	
C	-1.300		1.875	
DBC-64A	1.875		2.625	
DBC-65A	1.625			
C	-3.125		-1.125	1.875
DBC-66C	1.875		-1.375	
DBC-67A	-0.375		1.375	
B	1.875		-0.125	

	<u>Major</u>	<u>Major</u>	<u>Minor</u>	<u>Minor</u>
DBC- 68A	-1.625		-2.625	
c	-2.625		3.125	
DBC-71A	1.625			
B	1.125		-1.875	2.875
c	1.625		-3.625	
D	1.375			
DBC-72A	1.375			
B	1.625			
c	1.375		-2.625	
D	1.875			
DBC-73A	2.625		2.125	
B	2.625		2.125	
c	2.625		2.125	
DBC-75A	1.875		-3.875	0.125
B	1.875		-2.625	0.625
c	2.125		2.625	
D	1.875		2.625	
DBC- 76A	1.125			
B	1.625		-3.375	-2.625
c	1.375			
D	2.625			
DBC-77C	-0.375		-3.875	
DBC-78C	-0.625		-3.625	
DBC-79A	-3.875		-2.625	0.125
B	-3.875		-2.625	-0.375
c	-0.375		-3.875	-2.625
D	1.375			
DBC- 80A	-0.375		1.625	
c	0.900		1.700	-2.625
D	1.625			
DBC-81C	0.375		-1.375	-2.625
D	1.375			
DBC-82A	0.125		1.875	2.375
B	2.125			
c	1.875		-0.375	
D	0.625		1.875	
DBC-83A	2.125		2.625	
B	1.875		2.625	
c	1.875		-2.625	
D	2.625			

	<u>Major</u>	<u>Major</u>	<u>Minor</u>	<u>Minor</u>
DBC- 83A	2.125		2.625	
B	1.875		2.625	
c	1.875		-2.625	
D	2.625			
DBC-84B	2.125		2.625	
c	2.125		2.625	
D	2.625			
DBC- 85 ;				
Ykg-3C	1.875		-0.375	-2.875
D	2.125		1.375	
DBC-86A	2.625			
B	2.125		-0.900	-2.625
c	2.125	2.625	-3.125	
DBC-87A	0.125			
B	2.625		2.125	
c	2.625		2.125	-0.400
DBC-88A	-0.625		2.000	
B	-0.300		1.625	
c	-0.375		1.750	
DBC-89A	-2.625		-1.875	1.875
B	-0.265		2.625	
C	-1.375		2.625	
DBC-90A	2.625		2.000	-0.875
B	-1.125		2.000	
c	-1.375		-2.625	
D	1.875		2.625	
DBC-91A	0.375		1.625	2.625
B	0.375			
c	0.625		2.625	
D	0.875			
DBC-92A	1.375			
B	1.125			
c	0.700			
D	1.875		2.625	
DBC-93A	2.625		2.125	
DBC-101C	0.875		-2.625	
I)BC-102A	1.375		-3.875	
c	-1.375		-3.125	
DBC-103A	2.625		2.125	
B	2.625		2.125	
c	2.125		2.625	-3.875
DBC-104C	2.625		-3.125	3.875

		<u>Major</u>	<u>Major</u>	<u>Minor</u>	<u>Minor</u>
DBC-106A		-3.125	-2.625	-1.875	
PERMANENT PROFILES					
EG-1	A	2.125			
	B	2.125			
EG-3	C	2.125			
	D	2.125			
EG-4	A	2.125			
	B	2.125			
EG-8	A	1.625		2.125	3.125
	B	2.000			
	c	1.125	1.625		
Sr-1	A	1.875		1.375	
	B	1.700			
	c	0.875			
Ykg2	C	1.875			
	D	1.875			
Ykg3	C	1.875		-0.375	-2.875
	D	2.125		2.625	
Mal-2	B	1.875			
	D	1.125			
Mal-3	A	0.625			
	B	-2.625		-2.125	0.875
	c	0.125	-0.875	-2.125	-3.375
	D	-1.625		1.375	
Hq2	A	1.625			
	B	1.125		1.875	
	c	1.375			
	D	1.625		2.125	
Knk-1	A	2.625		3.125	
	B	1.375			
	C	3.215			
	D	3.125	2.625		
Ok-1	A	2.125			
Sea-1	A	1.875	1.375		
	B	1.700			
	c	0.875			

TABLE 3

COMPOSITIONAL ANALYSIS*

Copper River Province

	Qtz	F	Mica	Rf	Op
CA 1	56	5	5	28	6
2	57	2	5	27	9
3	53	1	7	34	5
4	48	5	4	32	11
5	60	2	5	23	10
6	60	2	9	23	6
7	55	2	4	27	12
8	53	8	0	31	8
9	54	8	3	33	2

Controller Bay Province

CA 10	44	6	10	37	3
11	45	11	7	35	2
12	24	4	3	68	1
13	46	4	4	44	2

Bering Glacier - Robinson Mountain Province

CA 14	7	4	0	89	0
15	2	0	0	98	0
16	0	0	0	100	0
17	4	0	0	96	0
18	10	0	1	89	0
19	21	0	2	77	0
20	7	0	0	93	0
21	20	1	0	79	0
22	14	1	0	85	0
23	58	3	1	38	0
24	28	4	1	66	1
25	14	0	0	86	0
26	15	0	0	84	1
27	59	3	0	26	12
28	46	1	0	50	3
29	2	0	0	98	0
30	47	5	0	44	4

Malaspina Foreland Province

CA 31	46	2	1	49	2
32	19	2	0	79	0
33	32	1	0	66	1
34	36	2	0	62	0
35	18	0	0	82	0
36	18	0	0	82	0
37	15	2	0	83	0
38	19	0	0	81	0

s

		Qt z	F	Mica	Rf	Op
CA	39	25	3	0	72	0
	40	11	1	0	88	0
	41	15	0	0	85	0
	42	19	0	0	81	0
	43	35	1	0	64	0
	44	21	1	0	78	0
	45	6	0	0	94	0
	46	28	0	0	72	0

Yakutat Foreland Province

CA	47	45	3	1	51	0
	48	40	6	3	51	0
	49	44	1	2	53	0
	50	45	3	1	51	0
	51	51	6	0	43	0
	52	39	8	0	53	0
	53	37	7	3	53	0
	54	49	4	1	47	0
	55	37	3	3	57	0
	56	41	5	3	49	2
	57	23	3	0	74	0
	58	17	0	0	83	0
	59	22	3	1	74	0

TABLE 4

MATURITY INDEX*

Copper River Province

	% Qtz	% Feld	% Rf	Maturity Index
CA 1	63	6	31	1.70
2	66	3	31	1.94
3	60	1	39	1.50
4	56	6	38	1.27
5	71	2	27	2.45
6	71	2	27	2.45
7	66	2	32	1.94
8	57	9	34	1.33
9	57	8	35	<u>1.33</u>
Mean	63.0	4*3	32.7	1.77
S.D.	5.87	2.95	4.27	0.46

Controller Bay Province

CA 10	51	7	42	1.04
11	50	12	38	1.00
12	25	4	71	0.33
13	50	4	46	<u>1.00</u>
Mean	44.0	6.7	49.3	0.84
S.C.	12.67	3.77	14.86	0.34

Bering Glacier - Robinson Mountain Province

CA 14	7	4	89	0.08
15	2	0	98	0.02
16	0	0	100	0.00
17	4	0	96	0.04
18	10	0	90	0.11
19	21	0	79	0.27
20	7	0	93	0.08
21	20	0	80	0.25
22	14	1	85	0.16
23	59	3	38	1.44
24	29	4	67	0.41
25	14	0	86	0.16
26	15	0	85	0.18
27	67	3	30	2.03
28	47	1	52	0.89
29	2	0	98	0.02
30	49	5	46	<u>0.96</u>
Mean	21.6	1.2	77.2	0.42
S.C.	21.18	1.79	22.33	0.58

Malaspina Foreland Province

	% Qtz	% Feld	% Rf	Maturity Index
CA 31	47	2	51	0.89
32	19	2	79	0.23
33	32	1	67	0.47
34	36	2	62	0.56
35	18	0	82	0.22
36	18	0	82	0.22
37	15	2	83	0.18
38	19	0	81	0.23
39	25	3	72	0.33
40	11	1	88	0.12
41	15	0	85	0.18
42	19	0	81	0.23
43	35	1	64	0.54
44	21	1	78	0.27
45	6	0	94	0.06
46	28	0	72	0.39
Mean	22.8	0.94	76.3	0.32
S.D.	10.52	1.00	10.98	0.21

Yakutat Foreland province

CA 47	45	3	52	0.82
48	41	6	53	0.69
49	45	1	54	0.81
50	45	3	52	0.81
51	5 1	6	43	1.04
52	39	8	53	0.64
53	38	7	55	0.51
54	49	4	47	0.96
55	38	3	59	0.61
56	42	5	53	0.72
57	23	3	74	0.30
58	17	0	83	0.20
59	22	3	75	0.28
Mean	38.1	4.0	57.9	0.65
S.D.	10.74	2.30	11.86	0.26